the FEBS Journal

www.febsjournal.org

Kinetic modelling of central carbon metabolism in *Escherichia coli*

Kirill Peskov, Ekaterina Mogilevskaya and Oleg Demin

DOI: 10.1111/j.1742-4658.2012.08719.x

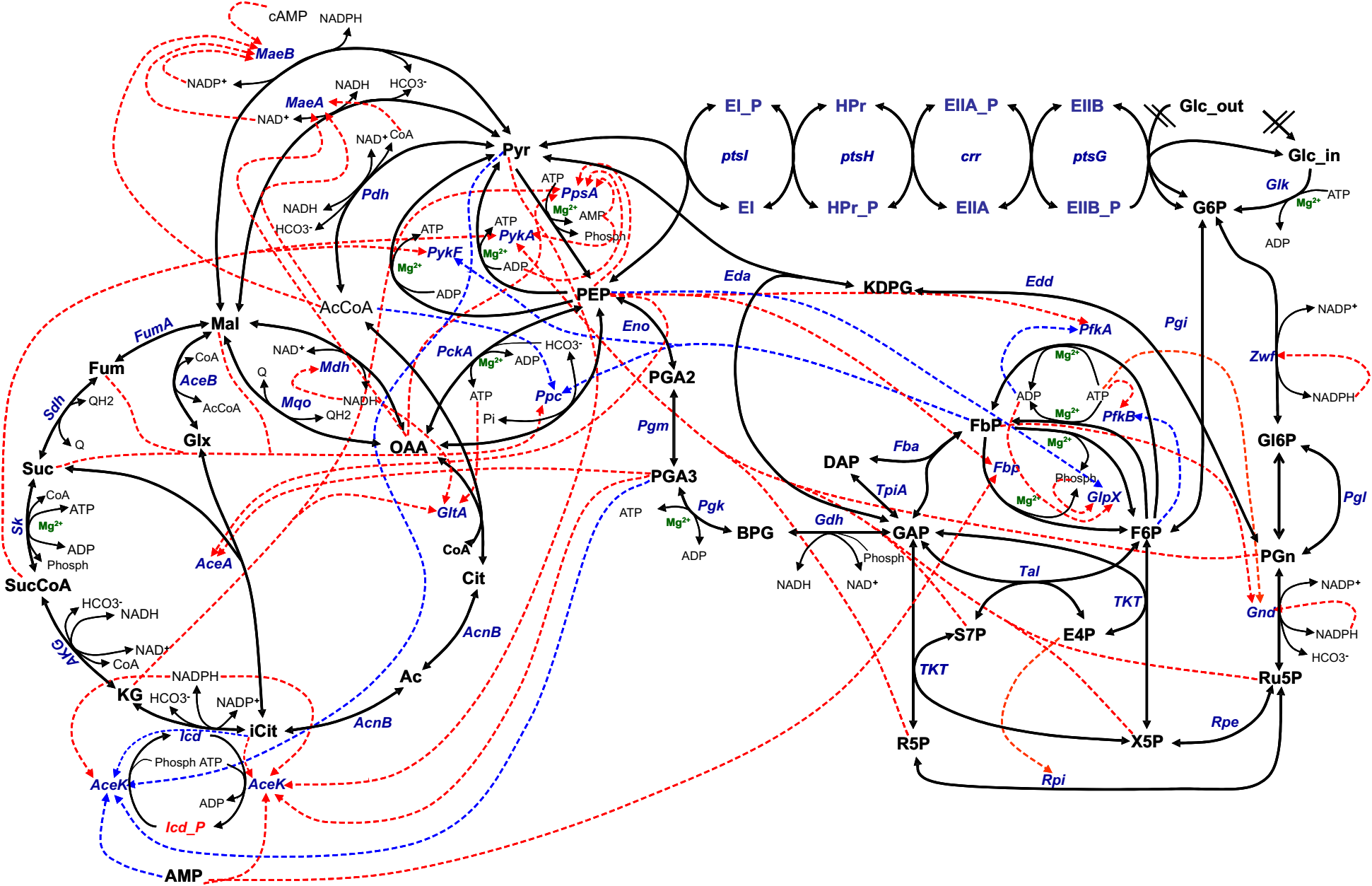
cAMP
NADPH
MaeB
NADP+
NADH
HCO3-
MaeA
NAD+
NAD+
CoA
Pyr
NADH
Pdh
HCO3-
ATP
PpsA
Mg2+
AMP
Phosph
ATP
PykA
PykF
Mg2+
ADP
Mg2+
ADP
AcCoA
PEP
EI_P
HPr
EIIA_P
EIIB
Glc_out
ptsI
ptsH
crr
ptsG
EI
HPr_P
EIIA
EIIB_P
Glc_in
Glk
ATP
Mg2+
ADP
G6P
Eda
KDPG
Edd
Eno
PfkA
Pgi
NADP+
Zwf
NADPH
FumA
Mal
NAD+
Mdh
NADH
PckA
Mg2+
ADP
HCO3-
PGA2
Fum
CoA
AceB
AcCoA
Q
Mqo
QH2
ATP
Pi
Ppc
Pgm
Mg2+
ATP
Sdh
QH2
Q
Glx
OAA
Suc
PGA3
Fba
DAP
TpiA
FbP
Mg2+
ADP
ATP
Mg2+
PfkB
Fbp
Mg2+
Phosph
GlpX
Mg2+
Gl6P
Pgl
CoA
ATP
Mg2+
ADP
Phosph
Sk
GltA
Pgk
Mg2+
ATP
ADP
BPG
Gdh
NADH
NAD+
Phosph
GAP
F6P
PGn
AceA
CoA
Cit
SucCoA
HCO3-
NADH
NAD+
CoA
AKG
AcnB
Tal
TKT
NADP+
NADPH
HCO3-
Gnd
S7P
E4P
TKT
Ac
NADPH
KG
HCO3-
NADP+
AcnB
Ru5P
Icd
Phosph ATP
AceK
AceK
ADP
Icd_P
iCit
Rpe
R5P
X5P
Rpi
AMP

Fig. S1. Scheme of metabolic regulation of *E. coli* central carbon metabolism. Enzymes participating in the pathway are shown by blue font, metabolites by black. Red dotted lines correspond to the inhibition, blue to the activation.

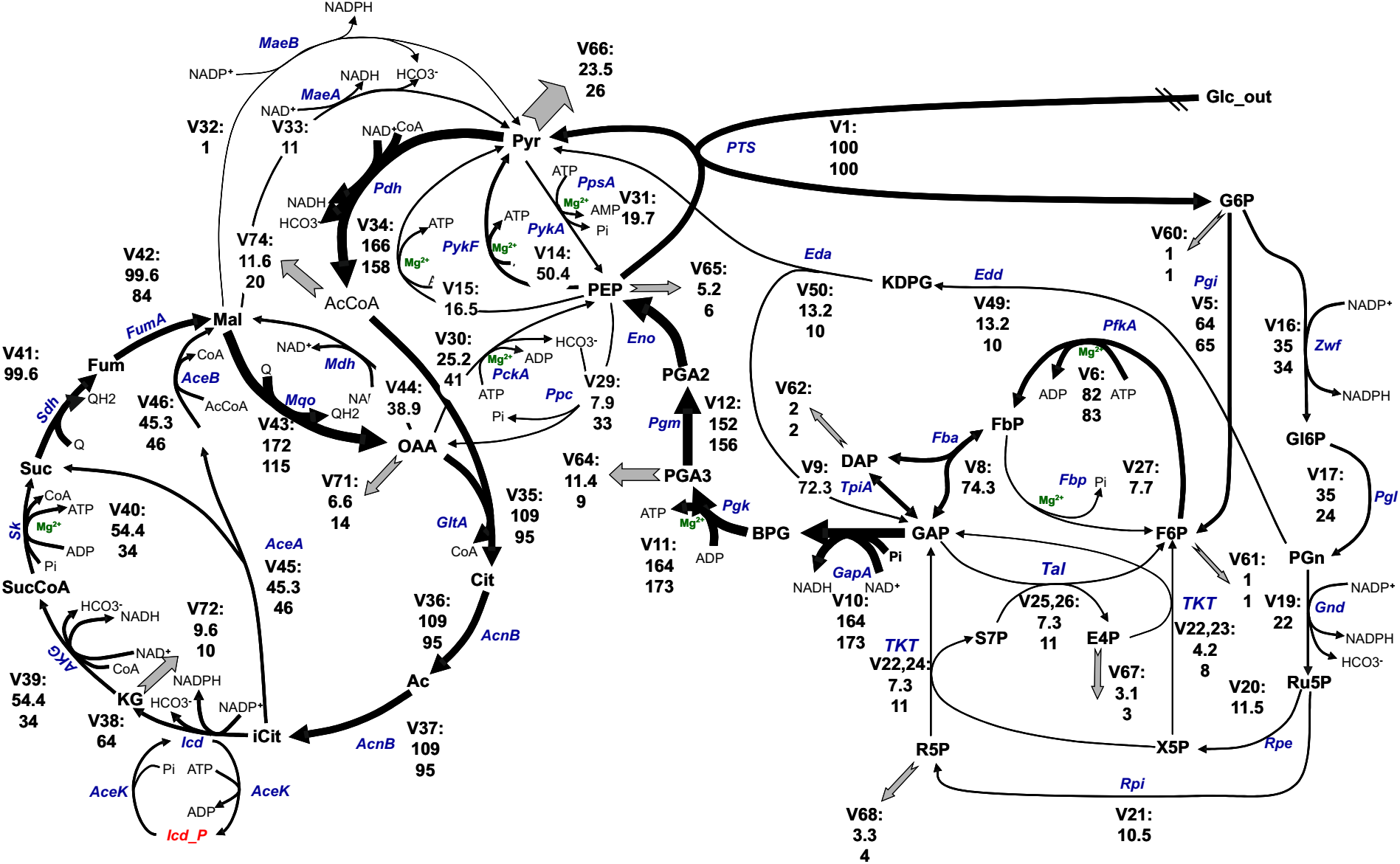
NADPH
MaeB
NADP+
NADH
HCO3-
MaeA
NAD+
V66:
23.5
26
V32:
1
V33:
11
NAD+CoA
Pyr
Glc_out
PTS
V1:
100
100
Pdh
NADH
HCO3-
V34:
166
158
ATP
PykF
Mg2+
ATP
PykA
Mg2+
V14:
50.4
ATP
PpsA
Mg2+
AMP
Pi
V31:
19.7
V74:
11.6
20
V42:
99.6
84
AcCoA
V15:
16.5
PEP
V65:
5.2
6
G6P
V60:
1
1
Eda
KDPG
Edd
V50:
13.2
10
V49:
13.2
10
Pgi
V5:
64
65
V16:
35
34
Zwf
NADP+
NADPH
PfkA
Mg2+
V6:
82
83
ADP
ATP
FbP
Gl6P
V17:
35
24
Pgl
V62:
2
2
Fba
DAP
V9:
72.3
TpiA
V8:
74.3
Fbp
Pi
Mg2+
V27:
7.7
F6P
PGn
V61:
1
1
V19:
22
Gnd
NADP+
NADPH
HCO3-
Ru5P
V20:
11.5
Rpe
X5P
R5P
Rpi
V68:
3.3
4
V21:
10.5
Tal
TKT
V22,23:
4.2
8
V25,26:
7.3
11
S7P
E4P
TKT
V22,24:
7.3
11
V67:
3.1
3
GAP
BPG
GapA
NADH
NAD+
Pi
V10:
164
173
Pgk
ATP
Mg2+
ADP
V11:
164
173
PGA3
V64:
11.4
9
Pgm
PGA2
Eno
V12:
152
156
V41:
99.6
Fum
FumA
Mal
V30:
25.2
41
Mg2+
PckA
HCO3-
ADP
ATP
V29:
7.9
33
Ppc
Pi
V65:
5.2
6
Sdh
QH2
Q
AceB
CoA
AcOA
NAD+
Mdh
Q
Mqo
NAD
QH2
V46:
45.3
46
V43:
172
115
V44:
38.9
OAA
V71:
6.6
14
Suc
Sk
CoA
ATP
Mg2+
ADP
Pi
V40:
54.4
34
SucCoA
GltA
CoA
V35:
109
95
Cit
AceA
V45:
45.3
46
V36:
109
95
AcnB
Ac
V72:
9.6
10
HCO3-
NADH
NAD+
CoA
AKG
V39:
54.4
34
KG
NADPH
HCO3-
NADP+
V38:
64
iCit
Icd
AcnB
V37:
109
95
AceK
Pi
ATP
ADP
AceK
Icd_P

Fig. S2. Scheme of predicted steady-state flux distribution in *E. coli* strain with knock out by the gene coding PykA aerobically grown in continuous culture and limiting concentration of carbon source. Under respective rate equation number there are a comparison between steady state values of fluxes and fluxomic data published by different authors [31,37,38]. Dimension of fluxes is mM/min.

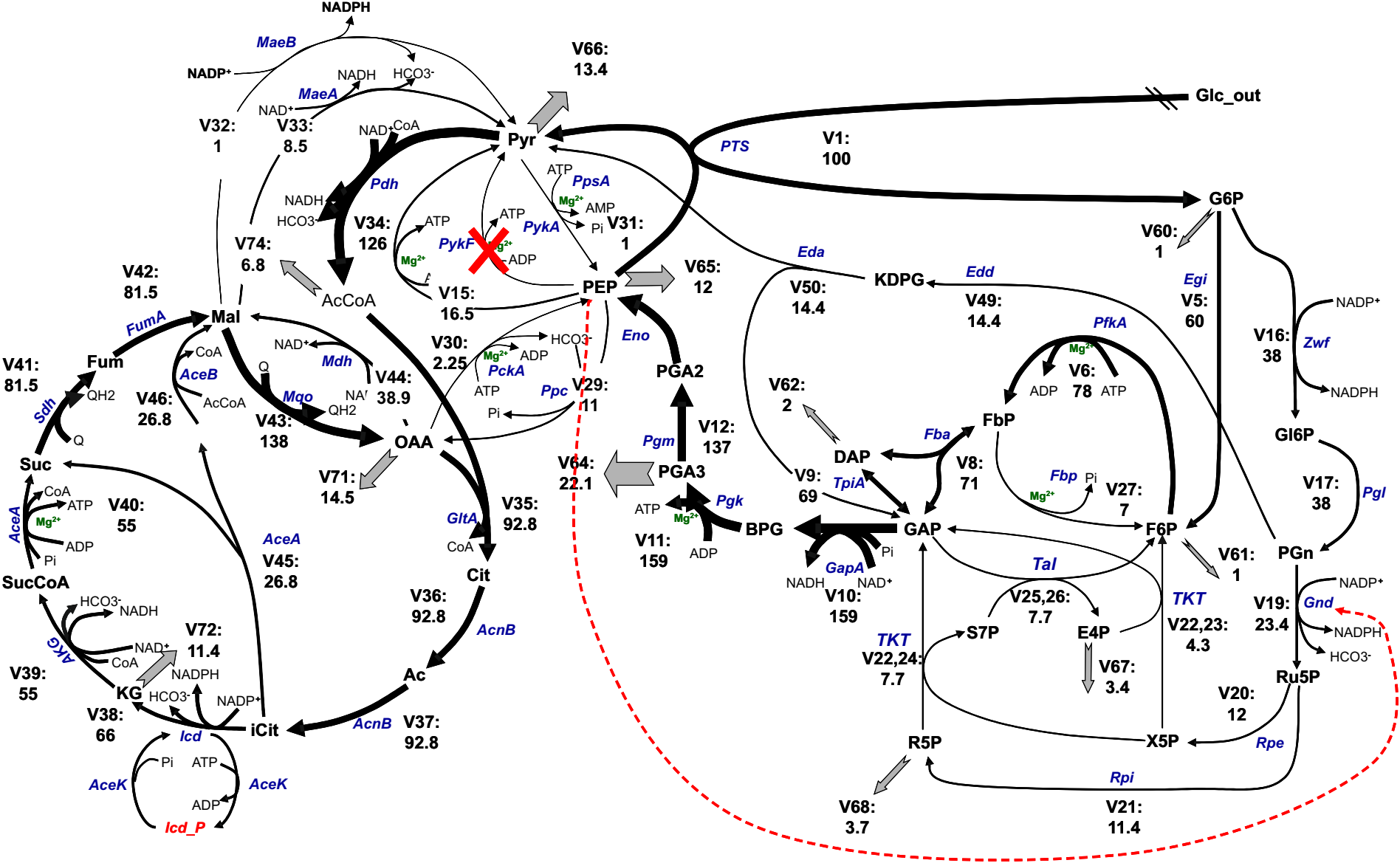
NADPH
MaeB
NADP+
NADH
HCO3-
MaeA
NAD+
V66:
13.4
V32:
1
V33:
8.5
NAD+
CoA
Pyr
Glc_out
PTS
V1:
100
Pdh
NADH
HCO3-
ATP
PpsA
Mg2+
AMP
Pi
V34:
126
ATP
ATP
PykA
V31:
1
V74:
6.8
PykF
Mg2+
ADP
G6P
V60:
1
Eda
V42:
81.5
AcCoA
V15:
16.5
PEP
V65:
12
KDPG
Edd
Egi
V5:
60
V50:
14.4
V49:
14.4
FumA
Mal
V30:
2.25
Mg2+
ADP
HCO3-
Eno
PfkA
NADP+
V16:
38
Zwf
NADPH
V41:
81.5
Fum
CoA
AceB
NAD+
Mdh
V44:
38.9
PckA
ATP
Ppc
V29:
11
PGA2
V6:
78
ADP
ATP
V62:
2
Sdh
QH2
Q
V46:
26.8
AcCoA
Mqo
V43:
138
Pi
FbP
Fba
Gl6P
V12:
137
Pgm
DAP
V8:
71
V17:
38
Pgl
Suc
OAA
V64:
22.1
PGA3
V9:
69
TpiA
Fbp
Pi
Mg2+
V27:
7
CoA
ATP
Mg2+
ADP
Pi
V40:
55
AceA
V71:
14.5
Pgk
ATP
Mg2+
ADP
BPG
GAP
F6P
V61:
1
PGn
AceA
V45:
26.8
GltA
V35:
92.8
CoA
V11:
159
Pi
GapA
NADH
NAD+
Tal
V10:
159
SucCoA
Cit
V25,26:
7.7
TKT
V22,23:
4.3
V19:
23.4
Gnd
NADP+
NADPH
HCO3-
HCO3-
NADH
V36:
92.8
AcnB
V72:
11.4
AKG
NAD+
CoA
NADPH
S7P
E4P
V39:
55
KG
HCO3-
NADP+
Ac
TKT
V22,24:
7.7
V67:
3.4
Ru5P
V38:
66
iCit
AcnB
V37:
92.8
Icd
V20:
12
R5P
X5P
Rpe
AceK
Pi
ATP
AceK
Rpi
ADP
V68:
3.7
V21:
11.4
Icd_P

Fig. S3. Scheme of predicted steady-state flux distribution in *E. coli* strain with knock out by the gene coding PykA aerobically grown in continuous culture and limiting concentration of carbon source. Under respective rate equation number there is predicted by the model 2 steady sate fluxes. Dimension of fluxes is mM/min.

Technical description of the kinetic model

ODE system, conservation laws, explicit functions, rate equations for recycling reaction and outputs

The kinetic model of *E. coli* CCM is determined using the following ODE system:

$$dG6P/dt = V_1 + V_2 + V_4 - V_5 - V_{16} - V_{60};$$
$$dGlc\_in/dt = V_3 - V_2 - V_4;$$
$$dF6P/dt = V_5 + V_{27} + V_{28} - V_6 - V_7 - V_{23} - V_{25} - V_{61};$$
$$dFbP/dt = V_6 + V_7 - V_8 - V_{27} - V_{28};$$
$$dGAP/dt = V_8 + V_9 + V_{22} + V_{25} + V_{50} - V_{10} - V_{63};$$
$$dDAP/dt = V_8 - V_9 - V_{62};$$
$$dBPG/dt = V_{10} - V_{11};$$
$$dPGA3/dt = V_{11} - V_{12} - V_{64};$$
$$dPGA2/dt = V_{12} - V_{13};$$
$$dPEP/dt = V_{13} + V_{30} + V_{31} - V_1 - V_2 - V_{14} - V_{15} - V_{29} - V_{65};$$
$$dPyr/dt = V_1 + V_2 + V_{14} + V_{15} + V_{32} + V_{33} + V_{50} - V_{31} - V_{34} - V_{66};$$
$$dGl6P/dt = V_{16} - V_{17} - V_{18};$$
$$dPGn/dt = V_{17} + V_{18} - V_{19} - V_{49};$$
$$dRu5P/dt = V_{19} - V_{20} - V_{21} - V_{70};$$
$$dR5P/dt = V_{21} + V_{24} - V_{68};$$
$$dX5P/dt = V_{20} - V_{22};$$
$$dE4P/dt = V_{23} + V_{26} - V_{67};$$
$$dS7P/dt = -V_{24} - V_{26} - V_{69};$$
$$dTkt/dt = -V_{22} - V_{23} - V_{24};$$
$$dTktc2/dt = V_{22} + V_{23} + V_{24};$$
$$dTal/dt = -V_{25} - V_{26};$$
$$dTalc3/dt = V_{25} + V_{26};$$
$$dKDPG/dt = V_{49} - V_{50};$$
$$dOAA/dt = V_{29} + V_{43} + V_{44} - V_{30} - V_{35} - V_{71};$$
$$dMal/dt = V_{42} + V_{46} - V_{32} - V_{33} - V_{43} - V_{44};$$

$$dCit/dt = V_{35} - V_{36};$$
$$dAco/dt = V_{36} - V_{37};$$
$$diCit/dt = V_{36} - V_{38} - V_{45};$$
$$dKG/dt = V_{38} - V_{39} - V_{72};$$
$$dSuc/dt = V_{40} - V_{41} + V_{45};$$
$$dFum/dt = V_{41} - V_{42};$$
$$dGlx/dt = V_{45} - V_{46};$$
$$dICD/dt = V_{48} - V_{47};$$
$$dICD\_P/dt = V_{47} - V_{48};$$
$$dAce/dt = V_{59} - V_{75};$$
$$dSucCoA/dt = V_{39} - V_{40} - V_{73};$$
$$dCoA/dt = V_{35} + V_{40} + V_{46} + V_{59} + V_{73} + V_{74} - V_{39} - V_{34};$$
$$dCoA/dt = V_{35} + V_{40} + V_{46} + V_{59} + V_{73} + V_{74} - V_{39} - V_{34};$$
$$dAcCoA/dt = V_{34} - V_{35} - V_{46} - V_{59} - V_{74};$$
$$dQ/dt = V_{54} - V_{41} - V_{43};$$
$$dQH_2/dt = -V_{54} + V_{41} + V_{43};$$
$$dNADPH/dt = V_{16} + V_{19} + V_{32} + V_{38} - V_{52} - V_{53};$$
$$dNADP/dt = -V_{16} - V_{19} - V_{32} - V_{38} + V_{52} + V_{53};$$
$$dNADH/dt = V_{10} + V_{33} + V_{34} + V_{39} + V_{44} - V_{51} + V_{53};$$
$$dNAD/dt = -V_{10} - V_{33} - V_{34} - V_{39} - V_{44} + V_{51} - V_{53};$$
$$dATP/dt = V_{11} + V_{40} + V_{14} + V_{15} + V_{56} - V_4 - V_6 - V_7 - V_{30} - V_{47} - V_{55} - V_{57};$$
$$dADP/dt = -V_{11} - V_{40} - V_{14} - V_{15} - V_{56} + V_4 + V_6 + V_7 + V_{30} + V_{47} + 2*V_{55};$$
$$dAMP/dt = -V_{55} + V_{31} + V_{58};$$
$$dcAMP/dt = V_{57} - V_{58};$$

We used simplified equations for the recycling and output reactions. These rate equations were derived using reversible or first-order mass action laws.

Recycling rate equations:

$$V_{51} = k^{+}_{rec\_NADH} * \left(NADH - NAD/K_{eq\_NADH} \right)$$

$$V_{52} = k^{+}_{rec\_NADPH} * \left(NADPH - {NADP}/{K_{eq\_NADPH}} \right)$$

$$V_{53} = k^{+}_{rec\_pnt} * \left(NAD * NADPH - {NADH * NADP}/{K_{eq\_pnt}} \right)$$

$$V_{54} = k^{+}_{rec\_Q} * \left(QH_2 - {Q}/{K_{eq\_QH2}} \right)$$

$$V_{55} = k^{+}_{rec\_adk} * \left(ATP * AMP - {ADP * ADP}/{K_{eq\_adk}} \right)$$

$$V_{56} = k^{+}_{rec\_ATPsynth} * \left(ADP * Phosph - {ATP}/{K_{eq\_ATPsynth}} \right)$$

$$V_{57} = k^{+}_{rec\_cyaA} * \left(ATP - {cAMP}/{K_{eq\_cyaA}} \right)$$

$$V_{58} = k^{+}_{rec\_cyaA} * \left(cAMP - {AMP}/{K_{eq\_cyaA}} \right)$$

$$V_{59} = k^{+}_{rec\_ATPsynth} * \left(AcCoA - {Ace * CoA}/{K_{eq\_ATPsynth}} \right)$$

Output reactions:

$$V_{60} = k_{out\_G6P} * G6P;\ V_{61} = k_{out\_F6P} * F6P;\ V_{62} = k_{out\_DAP} * DAP;$$

$$V_{63} = k_{out\_GAP} * GAP;\ V_{64} = k_{out\_PGA3} * PGA3;\ V_{65} = k_{out\_PEP} * PEP;$$

$$V_{66} = k_{out\_Pyr} * Pyr;\ V_{67} = k_{out\_E4P} * E4P;\ V_{68} = k_{out\_R5P} * R5P;$$

$$V_{69} = k_{out\_S7P} * S7P;\ V_{70} = k_{out\_Ru5P} * Ru5P;\ V_{71} = k_{out\_OAA} * OAA;\ V_{72} = k_{out\_KG} * KG$$

$$V_{73} = k_{out\_SucCoA} * SucCoA;\ V_{74} = k_{out\_AcCoA} * AcCoA;\ V_{75} = k_{out\_Ace} * Ace;$$

Conservation laws:

$$ATP_{tot} = ATP + ADP + AMP + cAMP;$$

$$ICD_{tot} = ICD + ICD\_P;$$

$$Q_{tot} = Q + QH_2;$$

$$CoA_{tot} = CoA + AcCoA + SucCoA;$$

$$Tal_{tot} = Tal + Talc3;$$

$$Tkt_{tot} = Tkt + Tktc3;$$

$$NAD_{tot} = NAD + NADH;$$

$$NAPD_{tot} = NADP + NADPH;$$

The following explicit functions were used to estimate the concentrations of magnesium complexes taking part as substrates in particular enzyme reactions:

$$ATPMg = {ATP * Mg}\Big/{\left(K_{d\_ATPMg} + Mg\right)};\quad ATP_f = {K_{d\_ATPMg} * Mg}\Big/{\left(K_{d\_ATPMg} + Mg\right)};$$

$$ADPMg = {ADP * Mg}\Big/{\left(K_{d\_ADPMg} + Mg\right)};\quad ADP_f = {K_{d\_ADPMg} * Mg}\Big/{\left(K_{d\_ADPMg} + Mg\right)};$$

$$FbPMg = {FbP * Mg}\Big/{\left(K_{d\_FbPMg} + Mg\right)};\quad FbP_f = {K_{d\_FbPMg} * Mg}\Big/{\left(K_{d\_FbPMg} + Mg\right)};$$

where ATPMg, ADPMg and FbPMg: concentration of magnesium complexes; ATP_f, ADP_f and FbP_f: concentrations of free metabolites, Mg: concentration of free magnesium ions; K_{d_ATPMg}, K_{d_ADPMg} and K_{d_FbPMg}: respective dissociation constants.

Values of the model parameters

Table 1S. Values of the parameters, which have been estimated against different *in vivo* experimental data on fluxomics, metabolomics and enzyme specific activity [S1,S4]. Model parameters, which appear in the rate equations of particular enzymes, are given in the section "*Kinetic models of the particular enzymes*" of this supplementary material.

Parameter	Value	Parameter	Value
K_{rec_NADH}	70 min^{-1}	V_{m_PTS}	22 mM/min
K_{eq_NADH}	12.6	V_{m_Pgi}	57 mM/min
K_{rec_NADPH}	400 min^{-1}	V_{mr_PfkA}	25 mM/min
K_{eq_NADPH}	12.3	V_{mr_PfkB}	25 mM/min
K_{rec_Pnt}	50 min^{-1}	V_{m_FbA}	437 mM/min
K_{eq_Pnt}	1.08	V_{m_Tpi}	510 mM/min
K_{rec_QH2}	500 min^{-1}	V_{m_Gdh}	50 mM/min
K_{eq_QH2}	15	V_{m_Pgk}	111 mM/min
K_{rec_adk}	3.4	V_{m_Pgm}	309 mM/min
K_{eq_adk}	1.13	V_{m_Eno}	23 mM/min
$K_{rec\_ATPsynth}$	1.5 min^{-1}	V_{mr_PykA}	10 mM/min
$K_{eq\_ATPsynth}$	2500	V_{mr_PykF}	24 mM/min
K_{rec_cyaA}	1.4 min^{-1}	V_{m_Zwf}	26 mM/min
K_{eq_cyaA}	0.0001	V_{m_Pgl}	750 mM/min
K_{rec_cpdA}	1000 min^{-1}	V_{m_Gnd}	8.5 mM/min
K_{eq_cpdA}	0.0001	V_{m_Rpe}	90 mM/min
K_{rec_AcCoA}	0 min^{-1}	V_{m_Rpi}	90 mM/min
K_{eq_AcCoA}	2.5	V_{m_Edd}	5 mM/min
		V_{m_Eda}	5 mM/min
K_{out_G6P}	0.0313 min^{-1}	V_{mr_Fbpase}	5 mM/min
K_{out_F6P}	0.131 min^{-1}	V_{m_GlpX}	0 mM/min
K_{out_DAP}	0.4 min^{-1}	V_{mr_Ppc}	4 mM/min
K_{out_GAP}	0 min^{-1}	V_{m_PckA}	15 mM/min
K_{out_PGA3}	0.3 min^{-1}	V_{m_PpsA}	4 mM/min
K_{out_PEP}	0.317 min^{-1}	V_{mr_MaeA}	100 mM/min
K_{out_Pyr}	0.74 min^{-1}	V_{mr_MaeB}	100 mM/min
K_{out_E4P}	1.47 min^{-1}	V_{m_Pdh}	20 mM/min
K_{out_S7P}	0 min^{-1}	V_{m_GltA}	486 mM/min
K_{out_R5P}	1.13 min^{-1}	V_{m_Acn1}	500 mM/min
K_{out_Ru5P}	0 min^{-1}	V_{m_Acn2}	500 mM/min
K_{out_OAA}	1.984 min^{-1}	V_{m_Icd}	30 mM/min
K_{out_KG}	3.57 min^{-1}	V_{m_Akg}	10.6 mM/min
K_{out_SucCoA}	0 min^{-1}	V_{m_Stc}	50 mM/min
K_{out_AcCoA}	5 min^{-1}	V_{m_Sdh}	45 mM/min
K_{out_Ace}	0 min^{-1}	V_{m_Fum}	37.2 mM/min
		V_{m_Mqo}	50 mM/min
		V_{m_Mdh}	99 mM/min
		V_{m_AceA}	8 mM/min
		V_{m_AceB}	12 mM/min
		V_{m_AceK}	2.5 mM/min

Table 2S. Values of the model parameters, which have been taken from the different literature sources. The initial concentrations of model variables have been taken from the literature [1S].

Parameter	Value (mM)	Literature source
Glc_out	0.0647	taken form [1S];
Mg^{2+}	1	taken form [2S];
Phosph	5	taken form [3S];
HCO^{3-}	10	taken form [3S];
ATP_{tot}	4.48	taken form [1S];
NAD_{tot}	1.57	taken form [1S];
$NADP_{tot}$	1.1	taken form [1S];
Q_{tot}	1	taken form [1S];
CoA_{tot}	0.5	taken form [1S];
ICD_{tot}	0.043	taken form [4S];
Tal_{tot}	0.006	taken form [5S];
Tkt_{tot}	0.007	taken form [6S];
K_{d_ATPMg}	0.0588	taken form [7S];
K_{d_ADPMg}	0.9	taken form [7S];
K_{d_FbPMg}	10	taken form [7S];
pH	7.5	taken form [3S];

Kinetic models of the particular enzymes

We used a standard approach for the development of kinetic models of particular enzymes. This approach can be subdivided into 5 steps.

1. Investigation of the catalytic and regulatory enzyme properties.
2. Development of the catalytic cycle scheme by considering the metabolic regulation.
3. Derivation of a rate equation by taking into account appropriate level of its detail. In the case of reversible enzymes we used rate equation, wherein V_{max} in forward direction is considered only. V_{max} in reverse direction, which is commonly hard to estimate from the published experimetal data, is not included in the rate equations. Instead, each rate equation includes $K_{eq,}$ which is implemented on the basis of Haldane relationships. K_{eq} is treated as independent parameter which value is identified on the basis of available experimental data. . The dependence of the enzyme rate on pH was taken into account by using the standard method described in the main text of this manuscript. All respective equations Z_{pH} (eq. 6 in the main text) and Q_{pH} (eq. 7 in the main text) are almost the same for most enzymes.
4. Verification of the model parameters. Depending on the available information parameter values can be obtained in the following ways: taken from literature sources or databases (EnzDB, BRENDA, EMP, WIT, etc.); calculated from values of other parameters; estimated from different experimental data about enzyme kinetics (measured *in vitro*); and assumed from general knowledge or model assumptions (free parameters). All literature sources that have been used during verification of the particular enzyme models are given in the tables of parameter values.
5. Model testing, analysis of behavior, and generation of predictions.

Simplified PTS rate equation

We have used simplified rate equations for the description of phosphotransferase system (PTS) functioning on the basis of the data published in [8S].

$$V_1 = \frac{V_{m\_PTS} * Glc\_out * PEP}{K_{m\_Glc\_out} * K_{m\_PEP} + K_{m\_Glc\_out} * PEP + K_{m\_PEP} * Glc\_out + Glc\_out * PEP}$$

$$V_2 = \frac{V_{m\_PTS} * Glc\_in * PEP}{K_{m\_Glc\_in} * K_{m\_PEP} + K_{m\_Glc\_in} * PEP + K_{m\_PEP} * Glc\_in + Glc\_out * PEP}$$

Values of the model parameters have been taken form literature and equal to 5 μM ($K_{m\_Glc\_out}$, $K_{m\_Glc\_in}$) and 0.3 mM (K_{m_PEP}) [9S]. All maximal rats of the reactions (Vm) are given in Table 1S of this supplementary material.

Models of glycolysis enzymes

Glycolysis consists of 10 reactions catalysed by 15 enzymes. There are more number of enzymes than reactions because of presence of isoforms, which duplicate 4 of enzymes. Most probably, that these enzymes are analogs of each other, because there are significant differences in their mechanisms of catalytic cycle and regulation. Nevertheless, we could develop separate kinetic models only for the isoenzymes of phosphofructokinase (PfkA and PfkB) and pyruvatekinase (PykA and PykF). This is because of lack of quantitative experimental information about the properties of other isoforms (such as FbaA and FbaB; PgmA, PgmB and PgmI). Therefore we used generic rate equations for Fba and Pgm reactions. Similarly, simplified descriptions using the first level of detailing were developed for enzymes such as Glk, Pgi, Fba, Gap, Pgk, Pgm and Eno. Kinetic models of PfkA, PfkB, PykA and PykF, which show allosteric properties, were developed using the third level of detailing. Therefore, we finally developed 11 kinetic models for glycolysis enzymes. The brief descriptions of these enzymes are presented below. Detailed descriptions of PfkA (V_6) and PfkB (V_7) were published earlier [10S,11S] and they are not given in this supplementary material.

Glucokinase (Glk).

The reaction catalysed by Glk does not play a main role in the overall flux of inflowing glucose phosphorylation. However, we considered this enzyme for the model, because it increases at particular metabolic conditions [12S]. We have used simplified Random Bi Bi rate equation for the Glk reaction.

$$V_4 = \frac{V_{m\_Glk} * Q_{pH\_Glk} * (Glc\_in * ATP - G6P * ADP / K_{eq\_Glk})}{K_{m\_Glc\_in} * K_{m\_ATP} + K_{m\_ATP} * Glc\_in + K_{m\_Glc\_in} * ATP + Glc\_in * ATP +}$$

$$+ K_{m\_Glc\_in} * K_{m\_ATP} * \left(G6P / K_{m\_G6P} + ADP / K_{m\_ADP} + G6P * ADP / K_{m\_G6P} * K_{m\_ADP} \right)$$

$$Q_{ph\_Glk} = \frac{1 + 2 * 10^{\left(pH_{m\_Glk} - pK_{\_Glk}\right)}}{1 + 10^{\left(pH - pK_{\_Glk}\right)} + 10^{\left(2 * pH_{m\_Glk} - pH - pK_{\_Glk}\right)}}$$

Parameter values and sources for verification are shown in table 3S.

Table 3S. Values of the Glk parameters.

Parameter	Value	Literature source
K_{eq_Glk}	20	Taken from [13S];
$pK_{\_Glk}$	10	Free parameter;
$pHm_{\_Glk}$	7.85	Estimated from [14S];
$K_{m\_Glc\_in}$	3.76 mM	Taken from [14S];
K_{m_ATP}	0.78 mM	Taken from [14S];
K_{m_ADP}	100 mM	Free parameter;
$K_{m\ G6P}$	100 mM	Free parameter;

Phosphoglucose isomerase (Pgi).

This enzyme catalyses reversible isomerization of G6P to F6P, therefore we described Pgi by reversible Michaelis-Menten equation with addition of PEP inhibition, which was observed recently [15S].

$$V_5 = \frac{V_{m\_Pgi} * Q_{pH\_Pgi} * (G6P - F6P / K_{eq\_Pgi})}{K_{m\_G6P} + G6P + K_{m\_G6P} * F6P / K_{m\_F6P} + K_{m\_G6P} * PEP / K_{ef\_PEP}}$$

$$Q_{ph\_Pgi} = \frac{1 + 2 * 10^{(pH_{m\_Pgi} - pK_{\_Pgi})}}{1 + 10^{(pH - pK_{\_Pgi})} + 10^{(2 * pH_{m\_Pgi} - pH - pK_{\_Pgi})}}$$

Parameter values and sources for verification are shown in table 4S.

Table 4S. Values of the Pgi parameters.

Parameter	Value	Literature source
K_{eq_Pgi}	0.4	Taken form [13S];
$pK_{\_Pgi}$	10	Estimated from [16S];
pH_{m_Pgi}	8.43	Estimated from [16S];
K_{m_G6P}	0.28 mM	Taken form [17S];
K_{m_F6P}	0.147 mM	Taken form [17S];
$K_{ef\ PEP}$	0.26 mM	Taken form [15S];

Fructose-1,6-bisphosphate aldolase (Fba).

This enzyme catalyses reaction of FbP cleavage with formation of GAP and DAP. As it was noted before we didn't provide separate rate equations for aldolase isoforms and used single rate equation. We described Fba by Ordered Uni Bi rate equation in accordance with Cleland's classification with additional inhibition by PEP, which was observed recently [15S].

$$V_8 = \frac{V_{m\_Fba} * Q_{pH\_Fba} * (FbP - GAP * DAP / K_{eq\_Fba})}{K_{m\_FbP} + FbP + K_{m\_FbP}\left(PEP / K_{ef\_PEP} + DAP / K_{m\_DAP} + GAP / K_{m\_GAP} + DAP * GAP / K_{m\_GAP} * K_{m\_DAP}\right)}$$

$$Q_{ph\_Fba} = \frac{1 + 2 * 10^{(pH_{m\_Fba} - pK_{\_Fba})}}{1 + 10^{(pH - pK_{\_Fba})} + 10^{(2 * pH_{m\_Fba} - pH - pK_{\_Fba})}}$$

Parameter values and sources for verification are shown in table 5S.

Table 5S. Values of the Fba parameters.

Parameter	Value	Literature source
K_{eq_Fba}	0.19	Taken from [18S];
$pK_{\_Fba}$	14.6	Estimated from [19S];
pH_{m_Fba}	10.92	Estimated from [19S];
K_{m_GAP}	0.13 mM	Taken from [20S];
K_{m_FbP}	0.12 mM	Taken from [19S];
K_{m_DAP}	0.13 mM	Taken from [19S];
$K_{ef\ PEP}$	1.85 mM	Taken from [15S];

Triose-phosphate isomerase (Tpi)

Tpi catalyses reaction of reversible isomerization, therefore this enzyme is described by reversible Michaelis-Menten equation.

$$V_9 = \frac{V_{m\_Tpi} * Q_{pH\_Tpi} * (DAP - GAP / K_{eq\_Tpi})}{K_{m\_DAP} + DAP + K_{m\_DAP} * GAP / K_{m\_GAP}}$$

$$Q_{ph\_Tpi} = \frac{1 + 2 * 10^{(pH_{m\_Tpi} - pK_{\_Tpi})}}{1 + 10^{(pH - pK_{\_Tpi})} + 10^{(2 * pH_{m\_Tpi} - pH - pK_{\_Tpi})}}$$

Parameter values and sources for verification are shown in table 6S.

Table 6S. Values of the Tpi parameters.

Parameter	Value	Literature source
K_{eq_Tpi}	0.04	Taken from [13S];
$pK_{\_Tpi}$	10	Estimated from [21S];
pH_{m_Tpi}	8.43	Estimated from [21S];
K_{m_GAP}	0.28 mM	Taken from [22S];
K_{m_DAP}	0.147 mM	Taken from [22S];

Glyceraldehyde-3-phosphate dehydrogenase (Gdh)

There is only one active form of Gdh in *E. coli* cells. We described Gdh by Random Bi Ter rate equation in accordance with Cleland's classification [23S].

$$V_{10} = \frac{V_{m\_Gdh} * Q_{pH\_Gdh} * (GAP * NAD * Phosph - BPG * NADH / K_{eq\_Gdh})}{Q_{pH\_Gdh} * K_{m\_GAP} * K_{m\_NAD} * K_{m\_Phosph} + K_{m\_NAD} * K_{m\_Phosph} * GAP + K_{m\_GAP} * K_{m\_Phosph} * NAD + K_{m\_GAP} * K_{m\_NAD} * Phosph + K_{m\_Phosph} * GAP * NAD + K_{m\_NAD} * GAP * Pi + K_{m\_GAP} * Phosph * NAD + GAP * NAD * Phosph + K_{m\_GAP} * K_{m\_NAD} * K_{m\_Phosph} * \left(BPG / K_{m\_BPG} + NADH / K_{m\_NADH} + BPG * NADH / K_{m\_BPG} * K_{m\_NADH} \right)}$$

$$Q_{pH\_Gdh} = \frac{1 + 2 * 10^{(pH_{m\_Gdh} - pK_{\_Gdh})}}{1 + 10^{(pH - pK_{\_Gdh})} + 10^{(2 * pH_{m\_Gdh} - pH - pK_{\_Gdh})}}$$

Parameter values and sources for verification are shown in table 7S.

Table 7S. Values of the Gdh parameters.

Parameter	Value	Literature source
K_{eq_Gdh}	20	Taken from [13S];
$pK_{\_Gdh}$	14.6	Estimated from [24S];
pH_{m_Gdh}	10.92	Estimated from [24S];
K_{m_GAP}	0.89 mM	Taken from [25S];
K_{m_NAD}	0.045 mM	Taken from [25S];
K_{m_Phosph}	0.53 mM	Taken from [25S];
K_{m_BPG}	0.2 mM	Taken from [26S];
K_{m_NADH}	0.012 mM	Taken from [26S];

Phosphoglycerate kinase (Pgk).

The first step of substrate phosphorylation is catalysed by Pgk. This enzyme functions by Random Bi Bi mechanism and does not have metabolic regulations. Therefore, we described Pgk by simplified Random Bi Bi rate equation derived using quasi steady-state method. However, its activity like for many other kinases depends on the presence of magnesium ions in the system, because the complex of ADP with Mg^{2+} becomes an actual substrate for this enzyme. We used explicit functions to take into account this enzyme's peculiarity. Therefore, in the model, $ATPMg^{2-}$ and $ADPMg^{2-}$ are explicit functions depending on ADP and Mg free concentrations (see the first part of this supplementary material). That is a general approach for considering the dependence of enzyme activity on magnesium ions, which we used for all enzymes, which have such peculiarity.

$$V_{11} = \frac{V_{m\_Pgk} * Q_{pH\_Pgk} * \left(BPG * ADPMg^{-} - PGA3 * ATPMg^{2-} \Big/ K_{eq\_Pgk}\right)}{K_{m\_BPG} * K_{m\_ADP} + K_{m\_ADP} * BPG + K_{m\_BPG} * ADPMg^{-} + BPG * ADPMg^{-} + \ldots}$$

$$\ldots + K_{m\_BPG} * K_{m\_ADP} * \left(PGA3 \Big/ K_{m\_PGA3} + ATPMg^{2-} \Big/ K_{m\_ATP} + PGA3 * ATPMg^{2-} \Big/ K_{m\_PGA3} * K_{m\_ATP} \right)$$

$$Q_{ph\_Pgk} = \frac{1 + 2 * 10^{\left(pH_{m\_Pgk} - pK_{\_Pgk}\right)}}{1 + 10^{\left(pH - pK_{\_Pgk}\right)} + 10^{\left(2 * pH_{m\_Pgk} - pH - pK_{\_Pgk}\right)}}$$

Parameter values and sources for verification are shown in table 8S.

Table 8S. Values of the Pgk parameters.

Parameter	Value	Literature source
K_{eq_Pgk}	100	Taken from [13S];
$pK_{\_Pgk}$	10	Estimated from [21S];
pH_{m_Pgk}	7.49	Estimated from [21S];
K_{m_BPG}	0.18 mM	Taken from [22S];
K_{m_ADP}	0.2 mM	Taken from [22S];
K_{m_PGA3}	1.28 mM	Taken from [22S];
K_{m_ATP}	0.48 mM	Taken from [22S];

Phosphoglycerate mutase (Pgm)

Pgm catalyses reaction of reversible isomerization, therefore this enzyme is described by reversible Michaelis-Menten equation.

$$V_{12} = \frac{V_{m\_Pgm} * Q_{pH\_Pgm} * (PGA3 - PGA2 / K_{eq\_Pgm})}{K_{m\_PGA3} + PGA3 + K_{m\_PGA3} * PGA2 / K_{m\_PGA2}}$$

$$Q_{ph\_Pgm} = \frac{1 + 2 * 10^{(pH_{m\_Pgm} - pK_{\_Pgm})}}{1 + 10^{(pH - pK_{\_Pgm})} + 10^{(2 * pH_{m\_Pgm} - pH - pK_{\_Pgm})}}$$

Parameter values and sources for verification are shown in table 9S.

Table 9S. Values of the Pgm parameters.

Parameter	Value	Literature source
K_{eq_Pgm}	0.1	Taken from [13S];
$pK_{\_Pgm}$	7.79	Free parameter;
pH_{m_Pgm}	7.28	Taken from [27S];
K_{m_PGA3}	1.1 mM	Taken from [27S];
K_{m_PGA2}	1.47 mM	Taken from [27S];

Enolase (Eno)

Eno catalyses reaction of reversible dehydration, therefore this enzyme is described by reversible Michaelis-Menten equation as well.

$$V_{13} = \frac{V_{m\_Eno} * Q_{pH\_Eno} * (PGA2 - PEP / K_{eq\_Eno})}{K_{m\_PGA2} + PGA2 + K_{m\_PGA2} * PEP / K_{m\_PEP}}$$

$$Q_{ph\_Eno} = \frac{1 + 2 * 10^{(pH_{m\_Eno} - pK_{\_Eno})}}{1 + 10^{(pH - pK_{\_Eno})} + 10^{(2 * pH_{m\_Eno} - pH - pK_{\_Eno})}}$$

Parameter values and sources for verification are shown in table 10S.

Table 10S. Values of the Eno parameters.

Parameter	Value	Literature source
K_{eq_Eno}	3	Taken from [13S];
$pK_{\_Eno}$	10	Free parameter;
pH_{m_Eno}	8.3	Taken from [28S];
K_{m_PGA2}	0.1 mM	Taken from [28S];
K_{m_PEP}	0.1 mM	Taken from [28S];

Pyruvatekinase-1 (PykF)

As mentioned before, there are 2 active pyruvatekinase isoforms in *E. coli* cells, PykF and PykA [29S-31S]. PykF has been considered the main pyruvatekinase, although the specific

activities of isoforms show that both enzymes have important roles during growth on the basic carbon substrates [30S]. The main biochemical PykF peculiarities are as follows:

1. PykF has an oligomeric structure (main form of the enzyme is a tetramer) [30S].
2. Dependence of PykF initial velocity on PEP concentration has a pronounced sigmoid shape [30S,32S,33S].
3. PykF can use both ADP and GDP as phosphate acceptor [30S].
4. PykF activity is strongly dependent on the concentration of magnesium ions, thereby showing that the true substrate of this reaction is a complex of ADP with Mg^{2+} [30S].
5. PykF has a complicated profile of metabolic regulation. Thus, FbB activates and SucCoA inhibits it [30S, 34S].
6. FbP has a regulatory binding site, which is structurally separated from the catalytic centre [35S].
7. Different FbP analogs can activate PykF as well [36S].
8. ADP inhibits enzyme activity at high substrate concentration [30S].
9. The dependence of maximal PykF activity on pH has an asymmetric shape [33S].

The main property of the enzymes is their allosteric character. Therefore, we are able to use the MWS approach for the correct description of the PykF peculiarities. Development of PykF model was based on generalisation of MWS approach, as proposed by Popova and Sel'kov [37S-40S]. The technical issues and a detailed description of the model development process can be found in our previous articles [10S,11S].

The rate equation of PykF monomer (*f*) at R-state can be represented in the following way:

$$f = \frac{V_{mr\_PykF} * \left(ADPMg^{-} * PEP \right)}{\left(1 + H^{+} / K_{h\_1} + K_{h\_2} / H^{+} \right) * Denom\_PykF\_r}$$

$$Denom\_PykF\_r = K_{ir\_PEP} * K_{mr\_ADPMg^{-}} + K_{mr\_ADPMg^{-}} * PEP +$$
$$+ K_{ir\_PEP} * K_{mr\_ADPMg^{-}} * \left(ADP_f / K_{ir\_ADP} + ADP_f * PEP / K_{ir\_ADP} * K_{ir\_PEP} \right) +$$
$$+ K_{mr\_PEP} * ADPMg^{-} + ADPMg^{-} * PEP +$$
$$+ K_{ir\_PEP} * K_{mr\_ADPMg^{-}} * \left(K_{mr\_ATPMg} * Pyr + K_{mr\_FbP} * ATPMg^{2-} + ATPMg^{2-} * Pyr \right)$$

The rate equation of PykF monomer at T-state (*f'*) has the analogous form but different parameter values. The Q function of PykF can be represented as follows:

$$Q = L_o * \left(\frac{\left(1 + FbP / K_{eft\_FbP} \right) * \left(1 + Suc\_coA / K_{eft\_Suc\_coA} \right)}{\left(1 + FbP / K_{efr\_FbP} \right) * \left(1 + Suc\_coA / K_{efr\_Suc\_coA} \right)} * \frac{E_r}{E_t} \right)^{n};$$

$$E_r = \frac{K_{ir\_PEP} * K_{mr\_ADPMg^-} * E_o}{Denom\_PykF\_r}; \qquad E_t = \frac{K_{it\_PEP} * K_{mt\_ADPMg^-} * E_o}{Denom\_PykF\_t};$$

where E_o, total enzyme concentration.

The complete PykF rate equation (V_{15}) can be obtained by substituting these equations in equation 4 in the main text of the manuscript. The final equation includes 31 parameters. The values and sensitivity ranges of the model parameters are given in table 11S.

Table 11S. Values of the PykF parameters.

Parameter	Value (mM)	Range of sensitivity (mM)	Literature source
K_{mr_ADPMg}	0.029	0.004 – 0.06	Estimated from [30S,34S];
K_{mr_GDPMg}	0.01	0.004 – 0.012	Estimated from [30S];
K_{mr_PEP}	3.48e-02	6.21e-03 – 6.02e-02	Estimated from [30S,34S];
K_{ir_PEP}	1.02	0.3 – 1.6	Estimated from [30S,34S];
K_{ir_ADP}	330	50 – ND [2]	Estimated from [30S,34S];
K_{ir_GDP}	4e-03	1.3e-03 – 7.1e-03	Estimated from [30S];
K_{efr_FbP}	0.049	0.042 – 0.055	Estimated from [30S,34S];
K_{efr_SucCoA}	500	40 – ND	Estimated from [34S];
K_{dr_Pyr}	100	ND	Free parameter;
K_{dr_ATP}	250	100 – 1000	Estimated from [34S];
$K_{dr\_ADP\_Pyr}$	100	ND	Free parameter;
K_{mt_ADPMg}	7.32e-06	1e-06 – 2.3e-05	Estimated from [30S,34S];
K_{mt_GDPMg}	0.011	0.005 – 0.014	Estimated from [30S];
K_{mt_PEP}	1.92	0.6 – 2.56	Estimated from [30S,34S];
K_{it_PEP}	50	4.64 – 95	Estimated from [30S,34S];
K_{it_ADP}	0.075	0.029 – 0.2	Estimated from [30S,34S];
K_{it_GDP}	3.7e-05	1.19e-05 – 5.27e-05	Estimated from [30S];
K_{eft_FbP}	700	100 – ND	Estimated from [30S,34S];
K_{efr_SucCoA}	5.37e-04	1.19e-04 – 9.8e-04	Estimated from [34S];
K_{dt_Pyr}	100	ND	Free parameter;
K_{dt_ATP}	5.89	0.2 – 25	Estimated from [30S];
$K_{dt\_ADP\_Pyr}$	100	ND	Free parameter;
L_o [1]	10^4	2e+03 – 4e+04	Estimated from [30S,34S];
ω [1]	10^4	ND	Estimated from [30S,34S];
n [1]	4	ND	Free parameter [30S];
K_{h_1}	2e-05	1e-05 – 3e-05	Estimated from [33S];
K_{h_2}	8.96e-05	5.7e-5 – 9.9e-5	Estimated from [33S];

[1] *- parameters L_0, ω, n are dimensionless.*

[2] *– range of sensitivity wasn't estimated.*

Pyruvatekinase-2 (PykA).

This isoform of pyruvatekinase was studied lesser than the first one. Only 2 studies have characterised the biochemical properties of this enzyme [31S,32S]. The main differences of

PykA from PykF are the metabolic regulatory profile (PykA is activated by AMP and the main intermediates of PMP) and strong specificity to ADP as the phosphate acceptor [31S,32S]. Other PykA peculiarities are the same as those for PykF. Because of these facts, we were able to use generalisation of the MWS approach to describe correctly the PykF peculiarities [37S-40S].

The rate equation of PykF monomer (*f*) at R-state can be represented by the following way:

$$f = \frac{V_{mr\_PykA} * \left(ADPMg^{-} * PEP \right)}{\left(1 + H^{+} / K_{h\_1} + K_{h\_2} / H^{+} \right) * Denom\_PykA\_r}$$

$$Denom\_PykA\_r = K_{ir\_PEP} * K_{mr\_ADPMg^{-}} + K_{mr\_ADPMg^{-}} * PEP +$$

$$+ K_{ir\_PEP} * K_{mr\_ADPMg^{-}} * \left(ADP_f / K_{ir\_ADP} + ADP_f * PEP / K_{ir\_ADP} * K_{ir\_PEP} \right) +$$

$$+ K_{mr\_PEP} * ADPMg^{-} + ADPMg^{-} * PEP +$$

$$+ K_{ir\_PEP} * K_{mr\_ADPMg^{-}} * \left(K_{mr\_ATPMg} * Pyr + K_{mr\_FbP} * ATPMg^{2-} + ATPMg^{2-} * Pyr \right)$$

The rate equation of PykF monomer at T-state (*f'*) has the analogous form but different parameter values. The Q function of PykF can be represented as follows:

$$Q = L_o * \left(\frac{1}{\left(1 + AMP / K_{efr\_AMP} + F6P / K_{efr\_F6P} + G6P / K_{efr\_G6P} + S7P / K_{efr\_S7P} + \right.} * \frac{E_r}{E_t} \right)^{n};$$
$$\left. + X5P / K_{efr\_X5P} + R5P / K_{efr\_R5P} + Ru5P / K_{efr\_Ru5P} \right)$$

$$E_r = \frac{K_{ir\_PEP} * K_{mr\_ADPMg^{-}} * E_o}{Denom\_PykA\_r}; \qquad E_t = \frac{K_{it\_PEP} * K_{mt\_ADPMg^{-}} * E_o}{Denom\_PykA\_t};$$

where E_o, total enzyme concentration.

The complete PykA rate equation (V_{14}) can be obtained by substituting these equations in equation 4 in the main text of the manuscript. The final equation includes 31 parameters. The values and sensitivity ranges of model parameters are given in table 12S.

Table 12S. Values of the PykA parameters.

Parameter	Value (mM)	Range of sensitivity (mM)	Literature source
K_{mr_ADPMg}	0.2	0.001 – 0.09	Estimated from [31S];
K_{mr_PEP}	1.1e-06	1.7e-07 – 8.52e-06	Estimated from [31S];
K_{ir_PEP}	0.084	0.003 – 0.97	Estimated from [31S];

K_{ir_ADP}	330	50 – ND [2]	Estimated from [31S];
K_{dr_Pyr}	100	ND	Free parameter;
K_{dr_ATP}	100	ND	Free parameter;
$K_{dr\_ADP\_Pyr}$	100	ND	Free parameter;
K_{mt_ADPMg}	8.48e-02	7.5e-03 – 2.3e-01	Estimated from [31S];
K_{mt_PEP}	0.054	0.002 – 0.47	Estimated from [31S];
K_{it_PEP}	0.83	0.02 – 5.2	Estimated from [31S];
K_{it_ADP}	0.314	0.0013 – 2.1	Estimated from [31S];
K_{dt_Pyr}	100	ND	Free parameter;
K_{dt_ATP}	100	ND	Free parameter;
$K_{dt\_ADP\_Pyr}$	100	ND	Free parameter;
K_{efr_AMP}	0.16	ND	Taken from [31S];
K_{efr_G6P}	0.08	ND	Taken from [31S];
K_{efr_F6P}	2	ND	Taken from [31S];
K_{efr_S7P}	0.1	ND	Taken from [31S];
K_{efr_X5P}	0.13	ND	Taken from [31S];
K_{efr_R5P}	0.001	ND	Taken from [31S];
K_{efr_Ru5P}	0.004	ND	Taken from [31S];
L_o [1]	25.3	1.4 – 57	Estimated from [31S];
ω [1]	10^4	ND	Estimated from [31S];
n [1]	4	ND	Taken from [31S];
K_{h_1}	1.71e-06	1e-06 – 3e-06	Estimated from [31S];
K_{h_2}	2.41e-02	1.7e-05 – 2.9e-05	Estimated from [31S];

[1] *- parameters L_0, ω, n are dimensionless.*

[2] *– range of sensitivity wasn't estimated.*

Models of pentose-monophosphate and Entner-Doudoroff pathways enzymes

PMP consists of 9 reactions catalysed by 10 enzymes. Rpi, Tkt and Tal are duplicated by isoforms. We used generic rate equations for these reactions, because of the lack of quantitative experimental data about enzyme properties. Additionally, Tkt and Tal show multiple activities; therefore, these reactions were described using the ODE subsystem considering enzyme states as variables. Moreover, we considered the presence of noncatalytic hydrolysis Gl6P for our model, because this process can have a physiological significance [41S]. The Entner-Doudoroff pathway consists of 2 supplementary reactions different from PMP and catalysed by two enzymes. Finally, for both pathways we developed 9 kinetic models of single enzymes using the first, second and fourth levels of detailing.

Glucose-6-phosphate dehydrogenase (Zwf).

The first step of PMP is an oxidation of G6P using $NADP^+$, which is the main Zwf cofactor at physiological conditions. Other Zwf biochemical properties are product inhibition with NADPH and functioning by Random mechanism [42S, 42S]. We described Zwf activity by Random Bi Ter rate equation in accordance with Cleland's classification.

$$V_{16} = \frac{V_{m\_Zwf} * \left(G6P*NADP - Gl6P * NADPH \Big/ K_{eq\_Zwf} \right)}{\left(1 + H^+ \Big/ K_{h\_1} + K_{h\_2} \Big/ H^+\right) * \left(\begin{array}{l} K_{d\_G6P} * K_{m\_NADP} + K_{m\_G6P} * NADP + K_{m\_NADP} * G6P + NADP * G6P + \\ + K_{d\_G6P} * K_{m\_NADP} * \left(\begin{array}{l} Gl6P \Big/ K_{d\_Gl6P} + NADPH \Big/ K_{d\_NADPH} + \\ + Gl6P * NADPH \Big/ K_{d\_Gl6P} * K_m^{NADPH} \end{array} \right) \end{array} \right)}$$

$$K_{eq\_Pgk} = \frac{V_{m\_Pgk} * K_{d\_Gl6P} * K_{m\_NADPH}}{V^r_{m\_Pgk} * K_{d\_G6P} * K_{m\_NADP}}$$

Parameter values and sources for verification are shown in table 13S.

Table 13S. Values of the Zwf parameters

Parameter	Value	Literature source
K_{eq_Zwf}	6e+10	Taken from [44S];
K_{h_1}	4.89e-04 mM	Estimated from [42S];
K_{h_2}	1.6e-07 mM	Estimated from [42S];
K_{m_G6P}	0.156 mM	Estimated from [42S, 43S];
K_{m_NADP}	0.0274 mM	Estimated from [42S, 43S];
K_{d_G6P}	0.192 mM	Estimated from [42S, 43S];
K_{m_Gl6P}	0.122 mM	Estimated from [42S, 43S];
K_{m_NADPH}	0.0168 mM	Estimated from [42S, 43S];
K_{d_Gl6P}	0.02 mM	Estimated from [42S, 43S];

6-phosphogluconolactonase (Pgl)

Pgl catalyses reaction of reversible dehydration of Gl6P, therefore this enzyme is described by reversible Michaelis-Menten equation.

$$V_{17} = \frac{V_{m\_Pgl} \cdot \left(Gl6P - PGn \Big/ K_{eq\_Pgl} \right)}{\left(1 + H^+ \Big/ K_{h\_1} + K_{h\_2} \Big/ H^+\right) * \left(K_{m\_Gl6P} + Gl6P + \frac{K_{m\_Gl6P}}{K_{m\_PGn}} \cdot PGn \right)}$$

$$K_{eq\_Pgl} = \frac{V_{m\_Pgl} * K_{m\_Pgn}}{V^r_{m\_Pgl} * K_{m\_Gl6P}}$$

Parameter values and sources for verification are shown in table 14S.

Table 14S. Values of the Pgl parameters

Parameter	Value (mM)	Literature source
K_{eq_Pgl}	42.8	Taken from [41S];
K_{h_1}	5.61e-03	Estimated from [45S];
K_{h_2}	9.73e-06	Estimated from [45S];
K_{m_Gl6P}	0.023	Taken from [46S];
K_{m_PGn}	10	Taken from [46S];

As reaction of hydrolysis can process spontaneously, we assumed rate equation for this reaction described by reversible mass action law and verified against data published in [41S].

$$V_{18} = K_{hyd\_Gl6P} * \left(Gl6P - PGn / K_{eq\_hyd\_Gl6P} \right)$$

where K_{hyd_Gl6P} equal to 0.01 min^{-1} and $K_{eq\_hyd\_Gl6P}$ to 42.8.

6-phosphogluconate dehydrogenase (Gnd).

The second NADP-dependent PMP step is catalased by Gnd. In spite of other PMP enzymes Gnd has several metabolic regulators, e. g. it is inhibited by FbP and ATP. Additionally, this enzyme has product inhibition by NADPH [47S,48S]. Analogously to Zwf we described Gnd activity by Random Bi Ter rate equation in accordance with Cleland's classification.

$$V_{19} = \frac{V_{m\_Gnd} * \left(PGn * NADP - Ru5P * NADPH * HCO3 / K_{eq\_Gnd} \right)}{Den\_Gnd * \left(1 + H^+ / K_{h\_1} + K_{h\_2} / H^+ \right)}$$

$$Den\_Gnd = K_{d\_\mathrm{PGn}} * K_{m\_NADP} + K_{m\_\mathrm{PGn}} * NADP + K_{m\_NADP} * \mathrm{PGn} + NADP * \mathrm{PGn} +$$

$$+ ATP * K_{d\_\mathrm{PGn}} * K_{m\_NADP} / K_{ef\_ATP} * \left(1 + ATP * PGn / K_{ef\_ATP\_PGn} \right) +$$

$$+ FbP * K_{d\_\mathrm{PGn}} * K_{m\_NADP} / K_{ef\_FbP} * \left(1 + FbP * NADP / K_{ef\_FbP\_NADP} \right) +$$

$$+ K_{d\_\mathrm{PGn}} * K_{m\_NADP} * \left(HCO_3 / K_{d\_HCO_3} + Ru5P / K_{d\_Ru5P} + NADPH / K_{d\_NADPH} + \right.$$

$$+ HCO_3 * Ru5P / K_{d\_HCO_3} * K_{d\_Ru5P} + HCO_3 * NADPH / K_{d\_HCO_3} * K_{d\_NADPH} +$$

$$\left. + NADPH * Ru5P / K_{d\_Ru5P} * K_{d\_NADPH} + NADPH * Ru5P * HCO_3 / K_{d\_HCO_3} * K_{d\_Ru5P} * K_{d\_NADPH} \right)$$

$$K_{eq\_Gnd} = \frac{V_{m\_Gnd} * K_{d\_HCO_3} * K_{d\_Ru5P} * K_{d\_NADPH}}{V^r_{m\_Gnd} * K_{d\_\mathrm{PGn}} * K_{m\_NADP}}$$

Parameter values and sources for verification are shown in table 15S.

Table 15S. Values of the Gnd parameters

Parameter	Value (mM)	Literature source
K_{eq_Gnd}	50	Taken form [49S];
K_{h_1}	5.76e-04	Estimated from [36S];
K_{h_2}	5e-07	Estimated from [36S];
K_{m_PGn}	0.033	Estimated from [36S];
K_{m_NADP}	0.015	Estimated from [36S];

K_{d_NADP}	0.117	Estimated from [36S];
$K_{ef\_ATP\_PGn}$	0.065	Estimated from [47S];
K_{ef_ATP}	0.14	Estimated from [47S];
K_{ef_FbP}	0.013	Estimated from [47S, 36S];
$K_{ef\_FbP\_NADPH}$	0.0052	Estimated from [47S, 36S];
K_{d_NADPH}	0.0034	Estimated from [47S, 36S];
K_{d_Ru5P}	0.044	Estimated from [47S, 36S];
K_{d_HCO3}	100	Free parameter;

During the model analysis, an additional version of the Gnd equation was derived. Based on the model assumption, we assumed the presence of additional metabolic regulation (model 2) and integrated it into the rate equation.

$$V_{19} = \frac{V_{m\_Gnd} * \left(PGn * NADP - Ru5P * NADPH * HCO3 / K_{eq\_Gnd} \right)}{Den\_Gnd * \left(1 + H^+ / K_{h\_1} + K_{h\_2} / H^+ \right) * \left(1 + PEP / K_{ef\_PEP} \right)}$$

The dissociation constant (K_{ef_PEP}) was assumed equal to 5 mM, based on the maximum coincidence with experimental data on steady state metabolomics.

Ribulose-phosphate 3-epimerase (Rpe).

Rpe catalyses reaction of reversible isomerization of Ru5P, therefore this enzyme is described by reversible Michaelis-Menten equation.

$$V_{20} = \frac{V_{m\_Rpe} \cdot \left(Ru5P - X5P / K_{eq\_Rpe} \right)}{\left(1 + H^+ / K_{h\_1} + K_{h\_2} / H^+ \right) * \left(K_{m\_Ru5P} + Ru5P + \frac{K_{m\_Ru5P}}{K_{m\_X5P}} \cdot X5P \right)}$$

Parameter values and sources for verification are shown in table 16S.

Table 16S. Values of the Rpe parameters

Parameter	Value (mM)	Literature source
K_{eq_Rpe}	1.5	Taken from [48S];
K_{h_1}	9.47e-04	Estimated from [48S];
K_{h_2}	1.02e-06	Estimated from [48S];
K_{m_Ru5P}	0.872	Estimated from [48S];
K_{m_X5P}	0.893	Estimated from [48S];

Ribose-5-phosphate isomerase (Rpi).

Rpi catalyses reaction of reversible isomerization of Ru5P, therefore this enzyme is described by reversible Michaelis-Menten equation. Additionally, this enzyme has one metabolic effector, E4P, therefore this peculiarity was added into the model account.

$$V_{21} = \frac{V_{m\_Rpi} \cdot \left(Ru5P - R5P / K_{eq\_Rpi} \right)}{\left(1 + H^+ / K_{h\_1} + K_{h\_2} / H^+ \right) * \left(K_{m\_Ru5P} + Ru5P + \frac{K_{m\_Ru5P}}{K_{m\_R5P}} \cdot R5P + \frac{K_{m\_Ru5P}}{K_{ef\_E4P}} \cdot E4P \right)}$$

Parameter values and sources for verification are shown in table 17S.

Table 17S. Values of the Rpi parameters

Parameter	Value (mM)	Literature source
K_{eq_Rpi}	0.33	Taken from [48S];
K_{h_1}	1.65e-04	Estimated from [51S];
K_{h_2}	1.05e-07	Estimated from [51S];
K_{m_Ru5P}	3.53e-03	Estimated from [52S];
K_{m_R5P}	1.23e-04	Estimated from [52S];
K_{ef_E4P}	0.67	Estimated from [50S];

Transketolase (Tkt).

Tkt catalyses the transfer of a two-carbon ketogroup from one carbohydrate (X5P, F6P, S7P) to another (GAP, E4P, R5P respectively). This enzyme does not have metabolic regulation and other complex biochemical peculiarities, but shows nontrivial catalytic mechanism and multiple activities. Therefore, we described Tkt with an ODE system, where variables are not only substrates but also enzyme states [5S].

The ODE system considering the Tkt multiple activities can be represented in the following way:

$$dTkt\_X5P / dt = -V_{22}; \; dTktc2\_GAP / dt = V_{22};$$
$$dTkt\_F6P / dt = -V_{23}; \; dTktc2\_E4P / dt = V_{23};$$
$$dTkt\_S7P / dt = -V_{24}; \; dTktc2\_R5P / dt = V_{24};$$

$$V_{22} = \frac{K_{cat\_X5P\_GAP} * (X5P * Tkt - GAP * Tktc2 / K_{eq\_X5P\_GAP})}{\left(1 + H^+ / K_{h\_1} + K_{h\_2} / H^+ \right)}$$

$$K_{eq\_X5P\_GAP} = K_{eq\_X5P} * K_{d\_X5P} / K_{d\_GAP}$$

$$V_{23} = \frac{K_{cat\_F6P\_E4P} * (F6P * Tkt - E4P * Tktc2 / K_{eq\_F6P\_E4P})}{\left(1 + H^+ / K_{h\_1} + K_{h\_2} / H^+ \right)}$$

$$K_{eq\_F6P\_E4P} = K_{eq\_F6P} * K_{d\_F6P} / K_{d\_E4P}$$

$$V_{24} = \frac{K_{cat\_S7P\_R5P} * (S7P * Tkt - R5P * Tktc2 / K_{eq\_S7P\_R5P})}{\left(1 + H^+ / K_{h\_1} + K_{h\_2} / H^+ \right)}$$

$$K_{eq\_S7P\_R5P} = {K_{eq\_S7P} * K_{d\_R5P}}/{K_{d\_S7P}}$$

Parameters values and sources for verification are shown in table 18S.

Table 18S. Values of the Tkt parameters

Parameter	Value	Literature source
K_{eq_X5P}	1	Taken from [53S];
K_{eq_F6P}	0.5	Estimated from [55S];
K_{eq_S7P}	0.33	Taken from [53S];
$K_{cat\_X5P\_GAP}$	7872 min^{-1}	Taken from [53S];
$K_{cat\_F6P\_E4P}$	4143 min^{-1}	Estimated from [55S];
$K_{cat\_S7P\_R5P}$	7872 min^{-1}	Taken from [53S];
K_{h_1}	1.24e-04 mM	Estimated from [54S];
K_{h_2}	4.5e-06 mM	Estimated from [54S];
K_{d_X5P}	0.022 mM	Estimated from [53S];
K_{d_R5P}	0.079 mM	Estimated from [53S];
K_{d_E4P}	0.001 mM	Estimated from [55S];
K_{d_GAP}	0.02 mM	Estimated from [53S];
K_{d_F6P}	0.07 mM	Estimated from [55S];
K_{d_S7P}	0.06 mM	Estimated from [53S];

Transaldolase (Tal).

Kinetic model describing Tal properties was developed using analogous to Tkt model assumptions. Only differences were in a number of possible enzyme activities and substrates (F6P and S7P as donors, E4P and GAP as acceptors respectively) and structure of transferred group [6S].

The ODE system considering the Tal multiple activities can be represented in the following way:

$${dTal\_F6P}/{dt} = -V_{25};\ {dTalc3\_GAP}/{dt} = V_{25};\ {dTal\_S7P}/{dt} = -V_{26};\ {dTalc3\_E4P}/{dt} = V_{26};$$

$$V_{25} = \frac{K_{cat\_F6P\_GAP} * (F6P * Tal - {GAP * Talc3}/{K_{eq\_F6P\_GAP}})}{\left(1 + {H^+}/{K_{h\_1}} + {K_{h\_2}}/{H^+}\right)}$$

$$K_{eq\_F6P\_GAP} = {K_{eq\_F6P} * K_{d\_F6P}}/{K_{d\_GAP}}$$

$$V_{26} = \frac{K_{cat\_S7P\_E4P} * (S7P * Tal - {E4P * Talc3}/{K_{eq\_S7P\_E4P}})}{\left(1 + {H^+}/{K_{h\_1}} + {K_{h\_2}}/{H^+}\right)}$$

$$K_{eq\_S7P\_E4P} = {K_{eq\_S7P} * K_{d\_F6P}}/{K_{d\_E4P}}$$

Parameter values and sources for verification are shown in table 19S.

Table 19S. Values of the Tal parameters

Parameter	Value	Literature source
K_{eq_F6P}	0.11	Taken from [6S];
K_{eq_S7P}	26.6	Estimated from [6S];
$K_{cat\_F6P\_GAP}$	4200 min^{-1}	Taken from [6S];
$K_{cat\_S7P\_E4P}$	2100 min^{-1}	Estimated from [6S];
K_{h_1}	4.43e-04 mM	Estimated from [56S];
K_{h_2}	1.9e-07 mM	Estimated from [56S];
K_{d_E4P}	0.025 mM	Estimated from [57S];
K_{d_GAP}	0.014 mM	Estimated from [57S];
K_{d_F6P}	0.333 mM	Estimated from [57S];
K_{d_S7P}	0.107 mM	Estimated from [57S];

6-phosphogluconate dehydratase (Edd).

Edd catalyses reaction of reversible dehydration of Gl6P. This enzyme does not have metabolic effectors, therefore this enzyme is described by reversible Michaelis-Menten equation.

$$V_{49} = \frac{V_{m\_Edd} * Q_{pH\_Edd} * (PGn - KDPG / K_{eq\_Edd})}{K_{m\_PGn} + PGn + K_{m\_PGn} * KDPG / K_{m\_KDPG}}$$

$$Q_{pH\_Edd} = \frac{1 + 2 * 10^{(pH_{m\_Edd} - pK\_Edd)}}{1 + 10^{(pH - pK\_Edd)} + 10^{(2 * pH_{m\_Edd} - pH - pK\_Edd)}}$$

Parameter values and sources for verification are shown in table 20S.

Table 20S. Values of the Edd parameters

Parameter	Value	Literature source
K_{eq_Edd}	1000	Taken from [58S];
pK_Edd	10	Free parameter;
pH_{m_Edd}	6.4	Taken from [58S];
K_{m_PGn}	0.6 mM	Taken from [58S];
K_{m_KDPG}	1 mM	Free parameter;

KDPG-aldolase (Eda).

Eda is described by simplified Ordered Uni Bi equation in accordance with Cleland's classification:

$$V_{50} = \frac{V_{m\_Eda} * Q_{pH\_Eda} * (KDPG - GAP * Pyr / K_{eq\_Eda})}{K_{m\_KDPG} + KDPG + K_{m\_KDPG} * \left(Pyr / K_{m\_Pyr}^{Pyr} + GAP / K_{m\_GAP} + Pyr * GAP / K_{m\_GAP} * K_{m\_Pyr} \right)}$$

$$Q_{pH\_Eda} = \frac{1 + 2 * 10^{(pH_{m\_Eda} - pK\_Eda)}}{1 + 10^{(pH - pK\_Eda)} + 10^{(2 * pH_{m\_Eda} - pH - pK\_Eda)}}$$

Parameter values and sources for verification are shown in table 21S.

Table 21S. Values of the Eda parameters

Parameter	Value	Literature source
K_{eq_Eda}	0.5	Taken from [59S];
$pK_{\_Eda}$	10	Free parameter;
pH_{m_Eda}	7.5	Taken from [59S];
K_{m_GAP}	1 mM	Free parameter;
K_{m_Pyr}	10 mM	Free parameter;
K_{m_KDPG}	0.35 mM	Taken from [59S];

Kinetic models of gluconeogenesis enzymes

Most of the gluconeogenesis enzymes are the same as those for glycolysis. Different enzymes were observed only for those reactions involving the irreversible glycolysis steps (e.g. phosphofructokinase and pyruvate kinase reactions). Finally, we developed 7 kinetic models for such enzymes: 4 using the third level of detailing, one with the second, and 2 with the first.

Fructosebisphosphatase-1 (Fbpase).

Fbpase is the main fructosebisphosphatase in *E. coli* cells. The activity of this gluconeogenesis enzyme was observed at growth on glucose as well [60S], where Fbp forms futile cycle together with Pfk enzymes. The other Fbpase biochemical peculiarities are as follows:

1. Fbpase has an oligomeric structure (main form of the enzyme is a tetramer) [61S-63S];
2. Enzyme activity has strong dependence on the concentration of magnesium ions. However, it is not completely clear which forms act as true substrates. Most probably, the free form of FbP and magnesium ions take these parts, whereas complex of FbP with magnesium plays the role of the competitive inhibitor [64S-67S];
3. AMP also competitively inhibits Fbpase by binding to the magnesium ions site [61S-64S].
4. Fbpase has allosteric regulation as well. PEP increase activity of this enzyme [61S-63S].

Most enzymes have an allosteric character. Because of this fact, we are able to use generalisation of the MWS approach for the correct description of Fbpase peculiarities. Development of Fbpase model was based on the generalisation of the MWS approach proposed by Popova and Sel'kov [37S-40S]. Our previous studies showed the technical issues and the model development process [10S,11S].

The rate equation of Fbpase monomer (*f*) at R-state can be represented in the following way:

$$f = \frac{V_{mr\_Fbpase} * FbP_f * Mg^{2+}}{Den\_Fbpase\_r * \left(1 + H^+ / K_{h\_1} + K_{h\_2} / H^+\right)}$$

$$Den\_Fbpase\_r = K_{ir\_FbP} * K_{mr\_Mg^{2+}} + K_{mr\_Mg^{2+}} * FbP_f + K_{mr\_FbP} * Mg^{2+} + FbP_f * Mg^{2+} +$$

$$+ K_{ir\_FbP} * K_{mr\_Mg^{2+}} * \left(\begin{array}{l} FbPMg / K_{ir\_FbPMg} + FbPMg * Mg^{2+} / K_{ir\_FbPMg} * K_{ir\_FbPMg\_Mg} + \\ + AMP / K_{ir\_AMP} + FbP_f * AMP / K_{ir\_AMP} * K_{ir\_AMP\_FbP} \end{array} \right) +$$

$$+ K_{ir\_FbP} * K_{mr\_Mg^{2+}} * \left(\begin{array}{l} Phosph / K_{ir\_Phosph} + F6P / K_{ir\_F6P} + Phosph * F6P / K_{ir\_Phosph} * K_{ir\_Phosph\_F6P} + \\ + Phosph * Mg^{2+} / K_{ir\_Phosph} * K_{mr\_Phosph\_Mg^{2+}} + F6P * Mg^{2+} / K_{ir\_F6P} * K_{mr\_F6P\_Mg^{2+}} + \\ + Phosph * F6P * Mg^{2+} / K_{ir\_Phosph} * K_{ir\_Phosph\_F6P} * K_{mr\_Phosph\_F6P\_Mg^{2+}} \end{array} \right)$$

The rate equation of Fbp monomer at T-state (*f'*) has the analogous form but different parameter values. The Q function of Fbp can be represented as follows:

$$Q = L_o * \left(\frac{\left(1 + PEP / K_{eft\_PEP}\right) * E_r}{\left(1 + PEP / K_{efr\_PEP}\right) * E_t} \right)^n;$$

$$E_r = \frac{K_{ir\_FbP} * K_{mr\_Mg^{2+}} * E_o}{Den\_Fbpase\_r}; \qquad E_r = \frac{K_{ir\_FbP} * K_{mr\_Mg^{2+}} * E_o}{Den\_Fbpase\_t};$$

where E_o – total enzyme concentration.

The complete Fbp rate equation (V_{27}) can be obtained by substituting these equations in equation 4 in the main text of the manuscript. The final equation includes 31 parameters. The values and sensitivity ranges of the model parameters are given in table 22S.

Table 22S. Values of the Fbp parameters.

Parameter	Value (mM)	Range of sensitivity (mM)	Literature source
K_{mr_Mg}	0.039	0.031 – 0.046	Estimated from [64S-67S];
K_{mr_FbP}	8.42e-03	6.21e-03 – 1.02e-02	Estimated from [64S-67S];
K_{ir_F6P}	1.12	0.88 – 1.37	Estimated from [64S-67S];
K_{ir_FbPMg}	0.76	0.55 – 0.93	Estimated from [64S-67S];
$K_{ir\_FbPMg\_Mg}$	0.356	0.17 – 0.57	Estimated from [64S-67S];
K_{ir_AMP}	1.22e-03	8.6e-04 – 1.69e-03	Estimated from [64S-67S];
$K_{ir\_AMP\_FbP}$	0.0256	0.0163 – 0.0389	Estimated from [64S-67S];
K_{efr_PEP}	0.45	0.28 – 0.69	Estimated from [61S];
K_{ir_F6P}	9.72	0.45 – 22.2	Estimated from [65S];
K_{ir_Phosph}	15.8	0.875 – 46	Estimated from [65S];

$K_{ir\_F6P\_Mg}$	0.385	0.024 – 6.78	Estimated from [65S];
$K_{ir\_F6P\_Phosph}$	6.6	0.67 – 48	Estimated from [65S];
$K_{ir\_Phosph\_Mg}$	0.856	0.031 – 16.5	Estimated from [65S];
$K_{ir\_F6P\_Phosph\_Mg}$	48.4	2.31 - 158	Estimated from [65S];
K_{mt_Mg}	55	44 – 67	Estimated from [65S];
K_{mt_FbP}	1e-05	ND – 5e-05	Estimated from [64S-67S];
K_{it_F6P}	6.89e-03	2.71e-03 – 9.47e-03	Estimated from [64S-67S];
K_{it_FbPMg}	6.42e-03	4.99e-03 – 8.63e-02	Estimated from [64S-67S];
$K_{it\_FbPMg\_Mg}$	100	24 – 230	Estimated from [64S-67S];
K_{it_AMP}	2.55e-04	1.09e-04 – 5.63e-04	Estimated from [64S-67S];
$K_{it\_AMP\_FbP}$	690	330 – 850	Estimated from [64S-67S];
K_{eft_PEP}	550	86 – ND	Estimated from [61S];
K_{it_F6P}	0.304	0.01 – 5.7	Estimated from [65S];
K_{it_Phosph}	3.21	0.1 – 15.5	Estimated from [65S];
$K_{it\_F6P\_Mg}$	315	45 – 812	Estimated from [65S];
$K_{it\_F6P\_Phosph}$	915	450 - 1680	Estimated from [65S];
$K_{it\_Phosph\_Mg}$	539	127 - 980	Estimated from [65S];
$K_{it\_F6P\_Phosph\_Mg}$	16.5	0.25 - 78	Estimated from [65S];
L_o [1]	8.15e-04	4.09e-04 – 9.72e-04	Estimated from [64S-67S];
ω [1]	10^4	ND [2]	Estimated from [64S-67S];
n [1]	4	ND	Taken from [68S];
K_{h_1}	7.51e-06	5.34e-06 – 9.12e-06	Estimated from [65S];
K_{h_2}	2.65e-05	1.7e-05 – 3.7e-05	Estimated from [65S];

[1] – *parameters L_0, W_r, W_t, ω, n are dimensionless.*

[2] – *range of sensitivity wasn't estimated.*

Fructosebisphosphatase-2 (GlpX).

Unfortunately, there is a lack of quantitative information about GlpX properties [63S]. Therefore, despite the evidences about allosteric properties we have to use the simplified approach (the level of detailing) for the derivation of its rate equation.

$$V_{28} = \frac{V_{m\_GlpX} * Q_{pH\_GlpX} * (FbP_f - F6P * Phosph / K_{eq\_GlpX})}{K_{m\_FbP} + FbP_f + K_{m\_FbP}\left(Phosph / K_{m\_Phosph} + F6P / K_{m\_Phosph} + Phosph * F6P / K_{m\_Phosph} * K_{m\_F6P}\right)}$$

$$Q_{pH\_GlpX} = \frac{1 + 2 * 10^{\left(pH_{m\_GlpX} - pK_{\_GlpX}\right)}}{1 + 10^{\left(pH - pK_{\_GlpX}\right)} + 10^{\left(2 * pH_{m\_GlpX} - pH - pK_{\_GlpX}\right)}}$$

Parameter values and sources for verification are shown in table 23S.

Table 23S. Values of the GlpX parameters.

Parameter	Value	Literature source
K_{eq_GlpX}	10^4	Taken from [69S];
$pK_{\_GlpX}$	14.6	Estimated from [65S];
pH_{m_GlpX}	10.92	Estimated from [65S];
K_{m_FbP}	0.025 mM	Taken from [69S];
K_{m_Phosph}	10 mM	Free parameter;

K_{m_F6P}	10 mM	Free parameter;

Phosphoenolpyruvate synthetase (PpsA)

PEP can be produced directly by using a single reaction with Pyr and ATP as substrates in *E. coli* cells. PpsA is an enzyme responsible for the catalysis of this reaction and has the following biochemical peculiarities:

1. PpsA acts by Ping Pong Uni Bi Bi Uni mechanism in correspondence to Cleland's classification [70S,71S]
2. True PpsA substrate is $ATPMg^{2-}$, the free form of ATP takes part as competitive inhibitor [71S]
3. Presence of magnesium ions in the catalytic site significantly increases the rate of the second reaction step [71S]
4. There is essential product inhibition by AMP and PEP [70S].
5. PpsA is also inhibited by ADP and TCA cycle intermediates, such as KG and OAA. Most probably, this inhibition has competitive character [70S].
6. The enzyme has different pH-optimums for forward and reverse reactions [72S].

A rate equation taking into account all the noted enzyme peculiarities can be expressed in the following way:

$$V_{31} = \frac{V_{m\_PpsA} * \left(ATPMg^{2-} * Pyr - AMP * PEP * Phosph * Mg^{2+} \Big/ K_{eq\_PpsA} \right)}{Z_S + Z_{SP} + Z_{SP}^{PEP} + Z_P + Z_I^{ATP} + Z_I^{ADP} + Z_I^{OAA} + Z_I^{KG}}$$

where $Z_S = Z_{pH}^S * \left(K_{m\_Pyr} * ATPMg^{2-} + Z_{Mg} * K_{m\_ATPMg} * Pyr + ATPMg^{2-} * Pyr \right)$

$$Z_P = W_{PpsA} \Big/ K_{eq\_PpsA} * \left(Z_{pH}^P * Z_P^1 + Z_{pH}^S * Z_P^2 \right)$$

$$Z_P^1 = Z_{Mg} * K_{d\_Mg} * K_{m\_Phosph} * AMP * PEP + Z_{Mg} * K_{d\_Mg} * K_{m\_AMP} * PEP * Phosph +$$
$$+ K_{d\_Mg} * K_{m\_Phosph} * AMP * Phosph * Mg^{2+} \Big/ K_{d\_Phosph} + AMP * PEP * Phosph * Mg^{2+}$$

$$Z_P^2 = K_{m\_PEP} * AMP * Phosph * Mg^{2+};$$

$$Z_I^{ATP} = Z_{pH}^S * \left(K_{m\_ATPMg} * Pyr * ATP_f \Big/ K_{ef\_ATP} + W_{PpsA} * K_{m\_PEP} * AMP * Phosph * Mg^{2+} * ATP_f \Big/ K_{ef\_ATP} * K_{eq\_PpsA} * Z_{Mg} \right)$$

$$Z_I^{ADP} = Z_{pH}^S * \left(K_{m\_ATPMg} * Pyr * ADP_f \Big/ K_{ef\_ADP} + W_{PpsA} * K_{m\_PEP} * AMP * Phosph * Mg^{2+} * ADP_f \Big/ K_{ef\_ADP} * K_{eq\_PpsA} * Z_{Mg} \right)$$

$$Z_I^{OAA} = Z_{pH}^S * \left(K_{m\_Pyr} * ATPMg^{2-} * OAA \Big/ K_{ef\_OAA} + W_{PpsA} * K_{m\_Phosph} * K_{d\_AMP} * K_{d\_Mg} * PEP * OAA * Z_{Mg} \Big/ K_{ef\_OAA} * K_{eq\_PpsA} \right)$$

$$Z_I^{KG} = Z_{pH}^S * \left(K_{m\_Pyr} * ATPMg^{2-} * KG \Big/ K_{ef\_KG} + W * K_{m\_Phosph} * K_{d\_AMP} * K_{d\_Mg} * PEP * KG * Z_{Mg} \Big/ K_{ef\_KG} * K_{eq\_PpsA} \right)$$

$$Z_{pH}^S = 1 + H^+ \Big/ K_{h\_S\_1} + K_{h\_S\_2} \Big/ H^+$$

$$Z_{pH}^P = 1 + H^+ \Big/ K_{h\_P\_1} + K_{h\_P\_2} \Big/ H^+$$

$$Z_{Mg} = 1 + Mg^{2+} \Big/ K_{d\_Mg}$$

Parameter values and sources for verification are shown in table 24S.

Table 24S. Values of the PpsA parameters.

Parameter	Value	Literature source
$K_{h\_S\_1}$	6.95e-07	Estimated from [72S];
$K_{h\_S\_2}$	1.43e-04	Estimated from [72S];
$K_{h\_P\_1}$	1.43	Estimated from [72S];
$K_{h\_P\_2}$	1.54e-08	Estimated from [72S];
W_{PpsA}	10	Taken from[72S];
K_{m_Pyr}	0.229	Estimated from [71S, 72S];
K_{m_ATPMg}	0.0549	Estimated from [71S, 72S];
K_{d_Pyr}	2740	Estimated from [71S, 72S];
K_{d_ATPMg}	0.1	Estimated from [71S, 72S];
K_{ef_ADP}	0.0283	Estimated from [70S, 72S];
K_{ef_ATP}	6.28e-04	Estimated from [70S, 72S];
K_{ef_KG}	0.274	Estimated from [70S, 72S];
K_{ef_OAA}	0.796	Estimated from [70S, 72S];
K_{m_PEP}	20.7	Estimated from [71S, 72S];
K_{m_AMP}	3.84e-04	Estimated from [71S, 72S];
K_{m_Phosph}	422	Estimated from [71S, 72S];
K_{d_Mg}	36.9	Estimated from [71S, 72S];
K_{d_PEP}	95.7	Estimated from [70S, 72S];
K_{d_AMP}	1480	Estimated from [71S, 72S];
K_{d_Phosph}	1730	Estimated from [70S, 72S];

Phosphoenolpyruvate carboxykinase (PckA).

This enzyme catalyses ADP-dependent carboxylation of PEP with formation of OAA. We described PckA activity by simplified Random Bi Ter rate equation in accordance with Cleland's classification.

$$V_{30} = \frac{V_{m\_PckA} * Q_{pH\_PckA} * (OAA * ATPMg * HCO_3 - {ADPMg * PEP}/{K_{eq\_PckA}})}{Q_{pH\_PckA} = \frac{1 + 2 * 10^{(pH_{m\_PckA} - pK_{\_PckA})}}{K_{m\_OAA} * K_{m\_ATPMg} * K_{m\_HCO3} + K_{m\_ATPMg} * K_{m\_HCO3} * OAA + K_{m\_OAA} * K_{m\_HCO3} * ATPMg}}$$

$$+K_{m\_OAA} * 10^{(pH - pK_{\_PckA})} * HCO_3 + K_{m\_HCO3} * OAA * ATPMg + K_{m\_ATPMg} * OAA * HCO_3 +$$

$$+K_{m\_OAA} * ATPMg * HCO_3 + OAA * ATPMg * HCO_3 +$$

$$+K_{m\_OAA} * K_{m\_ATPMg} * K_{m\_HCO3} * \left({ADPMg}/{K_{m\_ADPMg}} + {PEP}/{K_{m\_PEP}} + {ADPMg * PEP}/{K_{m\_ADPMg} * K_{m\_PEP}}\right)$$

Parameter values and sources for regulation are shown in table 25S.

Table 25S. Values of the PckA parameters.

Parameter	Value	Literature source
K_{eq_PckA}	1.88	Taken from [13S];
$pK_{\_PckA}$	10	Estimated from [73S];
pH_{m_PckA}	8	Estimated from [73S];
K_{m_OAA}	0.67 mM	Taken from [74S];
K_{m_ATPMg}	0.06 mM	Taken from [74S];
K_{m_HCO3}	13 mM	Taken from [74S];
K_{m_ADPMg}	0.05 mM	Taken from [74S];
K_{m_PEP}	0.07 mM	Taken from [74S];

Phosphoenolpyruvate carboxylase (Ppc).

Just like PcкA, Ppc catalyses PEP carboxylation with formation of OAA, although this reaction is not coupled with ADP phosphorylation. Because of this reaction the equilibrium is shifted to the OAA formation. Ppc reveals a number of allosteric properties, for example, sigmoid dependences of enzyme activity on substrate concentration, oligomeric structure, presence of regulatory sites for the enzymes effectors [75S-77S]. Therefore, we used the MWC approach for the derivation of Ppc rate equation [37S-40S].

The rate equation of Ppc monomer (*f*) at R-state can be represented in the following way:

$$f = \frac{V_{mr\_Ppc} * HCO_3 * PEP}{\left(1 + {H^+}/{K_{h\_1}} + {K_{h\_2}}/{H^+}\right) * Den\_Ppc\_r}$$

$$Denom\_Ppc\_r = K_{dr\_PEP} * K_{mr\_HCO_3^-} + K_{mr\_HCO_3} * PEP + K_{mr\_PEP} * HCO_3 + HCO_3 * PEP +$$

$$+K_{ir\_PEP} * K_{mr\_HCO_3} * \left({Phosph}/{K_{dr\_Phosph}} + {OAA}/{K_{dr\_OAA}} + {Phosph * OAA}/{K_{dr\_HCO_3} * K_{dr\_Phosph\_OAA}}\right)$$

The rate equation of Ppc monomer at T-state (*f'*) has the analogous form but different parameter values.

Based on the available information about Ppc regulation, we assumed that at the enzyme molecule, there are 2 regulatory sites—the activating site, wherein FbP and AcCoA bind, and the inhibiting site, wherein Mal, Suc, Cit, and Fum bind [77S]. Additionally, there are a number of contradictory data about the possible cooperative effects between some of these effectors. Nevertheless, these data are not sufficient for the model complication. Therefore, we did not consider this possible peculiarity; the final Q function for Ppc can be represented as follows:

$$Q = L_o * \left(\frac{\left(1 + Mal/K_{eft\_Mal} + Fum/K_{eft\_Fum} + Suc/K_{eft\_Suc} + Cit/K_{eft\_Cit}\right)}{\left(1 + FbP/K_{efr\_FbP} + AcCoA/K_{efr\_AcCoA}\right)} * \frac{E_r}{E_t} \right)^n$$

$$E_r = \frac{K_{dr\_PEP} * K_{mr\_HCO_3^-} * E_o}{Denom\_Ppc\_r}; \qquad E_t = \frac{K_{dt\_PEP} * K_{mt\_HCO_3^-} * E_o}{Denom\_Ppc\_t};$$

where E_o, total enzyme concentration.

The complete Ppc rate equation (V_{29}) can be obtained by by substituting these equations in equation 4 in the main text of the manuscript. The final equation includes 23 parameters. The values and sensitivity ranges of the model parameters are given in table 26S.

Table 26S. Values of the Ppc parameters.

Parameter	Value (mM)	Range of sensitivity (mM)	Literature source
K_{mr_HCO3}	0.002	ND – 0.29	Estimated from [75S-77S];
K_{mr_PEP}	3.2	1.08 – 5.57	Estimated from [75S-77S];
K_{dr_PEP}	655	245 – 870	Estimated from [75S-77S];
K_{dr_Phosph}	100	ND [2]	Free parameter;
K_{dr_OAA}	100	ND	Free parameter;
$K_{dr\_Phosph\_OAA}$	100	ND	Free parameter;
K_{mt_HCO3}	0.0022	ND – 0.31	Estimated from [75S-77S];
K_{mt_PEP}	5.12	2.98 – 7.47	Estimated from [75S-77S];
K_{dt_PEP}	0.0122	0.0013 – 0.2	Estimated from [75S-77S];
K_{dt_Phosph}	100	0.0013 – 2.1	Free parameter;
K_{dt_OAA}	100	ND	Free parameter;
$K_{dt\_Phosph\_OAA}$	100	ND	Free parameter;
K_{efr_FbP}	10	ND	Taken from [76S];
K_{efr_AcCoA}	0.14	ND	Taken from [76S];
K_{efr_Mal}	0.23	ND	Taken from [77S];
K_{efr_Suc}	23	ND	Taken from [77S];
K_{efr_Fum}	2.75	ND	Taken from [77S];
K_{efr_Cit}	34.4	ND	Taken from [77S];

L_o [1]	6.37e-06	1.4e-06 – 9.57e-06	Estimated from [75S-77S];
ω [1]	10^4	ND	Estimated from [31S];
n [1]	4	ND	Taken from [31S];
K_{h_1}	1.71e-06	1.01e-06 – 2.43e-06	Estimated from [75S];
K_{h_2}	6.1e-05	5.7e-05 –6.9e-05	Estimated from [75S];

[1] *- parameters L_0, ω, n are dimensionless.*

[2] *– range of sensitivity wasn't estimated.*

NAD-dependent malic enzyme (MaeA).

Malic enzymes catalyse the irreversible decarboxylation of Mal with the formation of Pyr. Overall, the catalytic properties of MaeA and MaeB quite similar and have allosteric character. The differences between the 2 malic enzymes are the cofactors and the metabolic effectors [78S]. For example, MaeA uses NAD as a cofactor and is activated by Asp and inhibited by ATP, CoA and AcCoA [79S-81S]. Moreover, MaeA activity is dependent on the concentration of magnesium ions.

The rate equation of MaeA monomer (*f*) at R-state can be represented in the following way:

$$f = \frac{V_{mr\_MaeA} * Mal * NAD * \left(1 + {Mg^{2+}}/{K_{dr\_Mg}}\right)}{\left(1 + {H^+}/{K_{h\_1}} + {K_{h\_2}}/{H^+}\right) * Den\_MaeA\_r}$$

$$Denom\_MaeA\_r = K_{dr\_NAD} * K_{mr\_Mal} + K_{mr\_Mal_3} * NAD + K_{mr\_NAD} * Mal + NAD * Mal +$$

$$+ K_{dr\_NAD} * K_{mr\_Mal} * \left({NADH}/{K_{dr\_NADH}} + {Pyr}/{K_{dr\_Pyr}} + {NADH * Pyr}/{K_{dr\_NADH} * K_{dr\_NADH\_Pyr}}\right);$$

The rate equation of MaeA monomer at T-state (f') has the analogous form but different parameter values. Based on the analogous assumptions as those for the Ppc model we proposed following Q function for MaeA:

$$Q = L_o * \left(\frac{\left(1 + {ASP}/{K_{eft\_Asp}} + {ATP}/{K_{eft\_ATP}}\right) * \left(1 + {AcCoA}/{K_{eft\_AcCoA}} + {CoA}/{K_{eft\_CoA}}\right) * E_r}{\left(1 + {ASP}/{K_{efr\_Asp}} + {ATP}/{K_{efr\_ATP}}\right) * \left(1 + {AcCoA}/{K_{efr\_AcCoA}} + {CoA}/{K_{efr\_CoA}}\right) * E_t} \right)^n$$

$$E_r = \frac{K_{dr\_NAD} * K_{mr\_Mal} * E_o}{Denom\_MaeA\_r}; \qquad E_t = \frac{K_{dt\_NAD} * K_{mt\_Mal} * E_o}{Denom\_MaeA\_t};$$

where E_o, total enzyme concentration.

The complete MaeA rate equation (V_{33}) can be obtained by by substituting these equations in equation 4 in the main text of the manuscript. The final equation includes 21 parameters. The values and sensitivity ranges of the model parameters are given in table 27S.

Table 27S. Values of the MaeA parameters.

Parameter	Value (mM)	Range of sensitivity (mM)	Literature source
K_{mr_MAl}	0.532	0.011 – 1.09	Estimated from [79S,80S];
K_{mr_NAD}	0.033	0.001 – 0.15	Estimated from [79S,80S];
K_{dr_NAD}	0.6	0.22 – 1.67	Estimated from [79S,80S];
K_{dr_Mg}	0.123	0.086 – 0.165	Estimated from [79S,80S];
K_{efr_Asp}	0.362	0.189 – 0.481	Estimated from [79S,80S];
K_{efr_ATP}	89	35 - ND	Estimated from [79S,80S];
K_{efr_AcCoA}	7.43	0.57 - ND	Estimated from [79S,80S];
K_{efr_CoA}	1.5	0.2 – 8.1	Estimated from [79S,80S];
K_{mt_Mal}	0.093	0.007 – 0.31	Estimated from [79S,80S];
K_{mt_NAD}	0.108	0.023 – 0.298	Estimated from [79S,80S];
K_{dt_NAD}	0.0837	0.00013 – 0.57	Estimated from [79S,80S];
K_{dt_Mg}	0.93	0.076 – 1.11	Estimated from [79S,80S];
K_{eft_Asp}	0.583	0.341 – 0.75	Estimated from [79S,80S];
K_{eft_ATP}	0.26	0.195 – 0.33	Estimated from [79S,80S];
K_{eft_AcCoA}	0.197	0.125 – 0.229	Estimated from [79S,80S];
K_{eft_CoA}	0.268	0.201 – 0.334	Estimated from [79S,80S];
L_o [1]	19.9	7.87 – 34.7	Estimated from [79S,80S];
ω [1]	10^4	ND	Estimated from [79S,80S];
n [1]	4	ND	Taken from [79S];
K_{h_1}	8.5e-07	5.09e-07 – 1.92e-06	Estimated from [81S];
K_{h_2}	2.82e-03	8.7e-04 –5.9e-03	Estimated from [81S];

[1] – *parameters L_0, ω, n are dimensionless.*

[2] – *range of sensitivity wasn't estimated.*

NADP-dependent malic enzyme (MaeB).

MaeB uses NADP as a cofactor and it is inhibited by ATP, AcCoA, cAMP and OAA [82S,83S]. In addition, product inhibition by NADP (and respective to this peculiarity inhibition by NAD) has been observed for MaeB as well [83S].

The rate equation of MaeB monomer (*f*) at R-state can be represented in the following way:

$$f = \frac{V_{mr\_MaeB} * Mal * NADP * \left(1 + Mg^{2+} / K_{dr\_Mg}\right)}{\left(1 + H^{+} / K_{h\_1} + K_{h\_2} / H^{+}\right) * Denom\_MaeB\_r}$$

$$Denom\_MaeB\_r = K_{dr\_NADP} * K_{mr\_Mal} + K_{mr\_Mal_3} * NADP * \left(1 + OAA / K_{efr\_OAA}\right) + K_{mr\_NADP} * Mal * \left(1 + NADH / K_{efr\_NADH}\right) +$$

$$+ NADP * Mal + K_{dr\_NADP} * K_{mr\_Mal} * \left(NADPH / K_{dr\_NADPH} + Pyr / K_{dr\_Pyr} + NADPH * Pyr / K_{dr\_NADPH} * K_{dr\_NADPH\_Pyr}\right);$$

The rate equation of MaeB monomer at T-state (f') has the analogous form but different parameter values. Based on the analogous assumptions as those for the Ppc model we proposed following Q function for MaeB:

$$Q = L_o * \left(\frac{\left(1 + cAMP/K_{eft\_cAMP}\right) * \left(1 + AcCoA/K_{eft\_AcCoA}\right) * E_r}{\left(1 + cAMP/K_{efr\_cAMP}\right) * \left(1 + AcCoA/K_{efr\_AcCoA}\right) * E_t} \right)^n;$$

$$E_r = \frac{K_{dr\_NADP} * K_{mr\_Mal} * E_o}{Denom\_MaeB\_r}; \qquad E_t = \frac{K_{dt\_NADP} * K_{mt\_Mal} * E_o}{Denom\_MaeB\_t};$$

where E_o, total enzyme concentration.

The complete MaeB rate equation (V_{32}) can be obtained by by substituting these equations in equation 4 in the main text of the manuscript. The final equation includes 23 parameters. The values and sensitivity ranges of the model parameters are given in table 28S.

Table 28S. Values of the MaeB parameters.

Parameter	Value (mM)	Range of sensitivity (mM)	Literature source
K_{mr_Mal}	3.71	3.11 – 4.29	Estimated from [82S,83S];
K_{mr_NADP}	0.0221	0.0134 – 0.305	Estimated from [79S,80S];
K_{dr_NADP}	0.0189	0.0012 – 0.415	Estimated from [79S,80S];
K_{dr_Mg}	8.22e-04	1.19e-04 –3.3e-04	Estimated from [84S];
K_{dr_NADPH}	0.011	0.009 – 0.18	Estimated from [82S,83S];
K_{efr_NADH}	0.0165	0.002 – 0.0269	Estimated from [82S,83S];
K_{efr_OAA}	7.06	5.51 – 9.49	Estimated from [82S,83S];
K_{efr_cAMP}	0.49	0.21 – 0.72	Estimated from [82S,83S];
K_{efr_AcCoA}	0.0635	0.0491 – 0.0782	Estimated from [82S,83S];
K_{mt_Mal}	3.28	2.76 – 3.75	Estimated from [82S,83S];
K_{mt_NADP}	0.0219	0.013 – 0.302	Estimated from [79S,80S];
K_{dt_NADP}	0.022	0.0025 – 0.049	Estimated from [79S,80S];
K_{dt_Mg}	0.124	0.023 – 0.21	Estimated from [84S];
K_{dt_NADPH}	0.043	0.017 – 0.077	Estimated from [82S,83S];
K_{eft_NADH}	0.015	0.0019 – 0.255	Estimated from [82S,83S];
K_{eft_OAA}	1.25e-03	7.5e-04 –1.98e-03	Estimated from [82S,83S];
K_{eft_cAMP}	1.57e-03	9.65e-04 –2.38e-03	Estimated from [82S,83S];
K_{eft_AcCoA}	2.19e-04	1.19e-04 –3.3e-04	Estimated from [82S,83S];
L_o [1]	0.134	0.047 – 0.225	Estimated from [82S,83S];
ω [1]	10^4	ND	Estimated from [82S,83S];
n [1]	6	ND	Taken from [82S];
K_{h_1}	3.43e-07	1.68e-07 – 5.93e-06	Estimated from [85S];
K_{h_2}	3.66e-05	1.81e-05 –5.99e-05	Estimated from [85S];

[1] – *parameters L_0, ω, n are dimensionless.*

[2] – *range of sensitivity wasn't estimated.*

Kinetic models of TCA cycle and glyoxylate bypass enzymes.

The TCA cycle and glyoxylate bypass totally consist of 13 reactions catalysed by 17 enzymes. As for the other CCM pathways, the number of enzymes is higher than the number of reactions because of the presence of isoforms. As for glycolysis, since these enzymes are analogs of each other, the isoforms can have essential differences in their catalytic or regulatory mechanisms. However, we did not develop separate rate equations for the TCA cycle enzymes, because of the lack of quantitative experimental information about particular isoforms. Moreover, genetic regulation respective to genes coding these enzymes does not allow simultaneous expression of isoforms. Therefore, production of the particular isoform is related to the specified culture phase or oxygen concentration [86S-88S], and the possibility of reaction duplication by isoform is minimised at a particular metabolic state.

Other kinetic models were mainly developed using the second level of detailing, although 2 enzymes were described by simplified equations (Mqo and AceB). Part of the TCA cycle enzymes, such as CS (V_{35}), ICD (V_{38}) and AceK (V_{47}, V_{48}) were described in detail in the previous articles [88S,89S].

Pyruvate dehydrogenase complex (Pdh).

Pdh is a multiprotein complex with a complex catalytic mechanism. Nevertheless, available experimental data show that the kinetic properties of this reaction can be successfully described by Ping Pong Ter Bi mechanism in accordance with the Cleland classification [23S]. The rate equation for this enzyme can be expressed in the following way:

$$V_{34} = \frac{V_m^{Pdh} * Q_{pH\_Pdh} * Pyr * NAD * CoA}{K_{m\_Pyr} * K_{m\_CoA} * NAD * \left(1 + Pyr/K_{m\_Pyr} + CoA/K_{m\_CoA} + NADH/K_{m\_NADH} + CoA/K_{m\_CoA} * NADH/K_{m\_NADH}\right) + \ldots}$$

$$\ldots + K_{m\_NAD} * Pyr * CoA * \left(1 + NAD/K_{m\_NAD} + AcCoA/K_{m\_AcCoA}\right) + K_m^{NAD} * K_m^{Pyr} * K_m^{CoA} * AcCoA/K_m^{AcCoA} * \left(1 + Pyr/K_m^{Pyr}\right)$$

$$\ldots + K_m^{NAD} * K_m^{Pyr} * K_m^{CoA} * NADH/K_{m\_NADH}\left(1 + AcCoA/K_{m\_AcCoA} + CoA/K_{m\_CoA} + CoA/K_m^{CoAr} * AcCoA/K_m^{AcCoA}\right)$$

$$Q_{ph\_Pdh} = \frac{1 + 2 * 10^{(pHm\_Pdh - pK\_Pdh)}}{1 + 10^{(pH - pK\_Pdh)} + 10^{(2 * pHm\_Pdh - pH - pK\_Pdh)}}$$

The values of parameters and sources of verification are shown in table 29S.

Table 29S. Values of the Pdh parameters.

Parameter	Value	Literature source
$pK_{\_Pdh}$	10	Free parameter;
pH_{m_Pdh}	6.8	Estimated from [91S];
K_{m_Pyr}	0.26 mM	Taken from [91S];
K_{m_NAD}	0.01 mM	Estimated from [90S];
K_{m_CoA}	0.005 mM	Estimated from [90S];
K_{m_AcCoA}	0.005 mM	Estimated from [90S];
K_{m_NADH}	0.01 mM	Free parameter;

Aconitase (AcnB)

This enzyme is coded by the *acnB* gene and it catalyses isocitrate formation from citrate through aconitate. There are 3 isoforms of aconitases in *E. coli*. The 2 main enzymes are aconitase A (*acnA*) and B (*acnB*), and the minor one is aconitase C (*acnC*) [92S]. AcnA expression is induced by Fe ions and other events related to oxidative stress during stationary phase of growth. AcnB is the main enzyme at the exponential phase of culture growth. We considered only AcnB isoform for the model. Both steps of the reaction were described as one substrate-one product reactions catalysed by the same enzyme. Rate equations were included into the model as follows:

$$V_{35} = V_{m\_Acn1}\frac{Cit - Aco/K_{eq\_Acn1}}{K_{m\_Cit}(1+\frac{Aco}{K_{m\_Aco}}+\frac{iCit}{K_{m\_iCit}})+Cit};\ V_{36} = V_{m\_Acn2}\frac{K_{eq\_Acn2}(Aco - iCit/K_{eq\_Acn2})}{K_{m\_iCit}(1+\frac{Aco}{K_{m\_Aco}}+\frac{Cit}{K_{m\_Cit}})+iCit}$$

Parameter values and sources for verification are shown in table 30S.

Table 30S. Values of the AcnB parameters.

Parameter	Value	Literature source
K_{m_Cit}	11.2mM	Estimated from [92S]
K_{m_Aco}	0.02mM	Estimated from [92S]
K_{m_iCit}	0.01mM	Free parameter
K_{eq_Acn1}	0.032	Estimated from [93S]
K_{eq_Acn2}	2.615	Estimated from [93S]

Alpha-Ketoglutarate Dehydrogenase (Akg)

The rate equation for this enzyme was derived from the irreversible Ping Pong mechanism with cooperative interaction between 2 catalytic sites since Akg shows alpha-ketoglutarate (KG) inhibition at concentration higher than 0.08 mM [94S]. A detailed description

of the AKG model development can be found in our previous article [89S]. According to available experimental data [95S] only the maximal rate depends on pH. The rate equation was included into the model as follows:

$$V_{39} = \frac{V_{Akg}}{(1+\frac{H}{K_{h\_1}}+\frac{K_{h\_2}}{H})} * \frac{KG^2 * CoA * NAD}{KG^2 * CoA * NAD + KG^2 * k_{4\_Akg}k_{3\_Akg} * NAD * K_{d\_CoA} / (k_{2\_Akg}k_{3\_Akg} + k_{4\_Akg}k_{3\_Akg} + k_{2\_Akg}k_{4\_Akg}) + k_{2\_Akg}k_{4\_Akg}KG^2 * CoA * K_{d\_NAD} / (k_{2\_Akg}k_{3\_Akg} + k_{4\_Akg}k_{3\_Akg} + k_{2\_Akg}k_{4\_Akg}) + KG * CoA * NAD * K_{2\_KG} + KG * NAD * K_{2\_KG}K_{d\_CoA}k_{1\_Akg}k_{3\_Akg} / (k_{2\_Akg}k_{3\_Akg} + k_{4\_Akg}k_{3\_Akg} + k_{2\_Akg}k_{4\_Akg}) + KG * CoA * K_{2\_KG}K_{d\_NAD}k_{1\_Akg}k_{2\_Akg} / (k_{2\_Akg}k_{3\_Akg} + k_{4\_Akg}k_{3\_Akg} + k_{2\_Akg}k_{4\_Akg}) + CoA * NAD * K_{1\_KG}K_{2\_KG}k_{3\_Akg}k_{2\_Akg}} + \frac{V_{0.08\_Akg} * KG * CoA * NAD}{KG * CoA * NAD + KG * NAD * K_{m\_CoA} + KG * CoA * K_{m\_NAD} + CoA * NAD * K_{m\_KG}}$$

where $V_{0.08\_Akg}$ is the maximal rate with 0.08 mM of alpha-ketoglutarate.

Parameter values and sources for verification are shown in table 31S.

Table 31S. Values of the Akg parameters.

Parameter	Value	Literature source
K_{m_KG}	0.02 mM	Estimated from [94S];
K_{m_CoA}	0.076 mM	Estimated from [94S];
K_{m_NAD}	0.098 mM	Estimated from [94S];
K_{2_KG}	0.25mM	Estimated from [94S];
$V_{0.08\_Akg}$	21.2mM/min	Estimated from [94S];
k_{1_Akg}	1e5 1/min	Estimated from [94S]
k_{2_Akg}	1e7 1/min	Estimated from [94S]
k_{3_Akg}	1e6 1/min	Estimated from [94S]
k_{4_Akg}	5e4 1/min	Estimated from [94S]
K_{1_KG}	0.05mM	Estimated from [94S]
K_{d_CoA}	0.07mM	Estimated from [94S]
K_{d_NAD}	0.08mM	Estimated from [94S]
K_{h_1}	2.3e-5 mM	Estimated from [95S]
K_{h_2}	1.5e-7 mM	Estimated from [95S]

Succinate Dehydrogenase (Sdh)

Sdh is a multiprotein complex which catalyses succinate oxidation to fumarate with coenzyme Q reducing. The rate equation was taken according to Random Bi Bi mechanism:

$$V_{41} = \frac{V_{m\_Sdh} * \left(Suc * Q - Fum * QH_2 \Big/ K_{eq\_Sdh} \right)}{\left(1 + H^+ \Big/ K_{h\_1} + K_{h\_2} \Big/ H^+ \right) * \left(\begin{array}{l} K_{d\_Suc} * K_{m\_Q} + Suc * K_{m\_Q} + Q * K_{m\_Suc} + Suc * Q + \\ + K_{d\_Suc} * K_{m\_Q} \left(\dfrac{Fum}{K_{ef\_Fum}} + \dfrac{QH_2}{K_{m\_QH_2}} \dfrac{K_{m\_Fum}}{K_{ef\_Fum}} + \dfrac{Fum}{K_{ef\_Fum}} \dfrac{QH_2}{K_{m\_QH_2}} \right) \end{array} \right)};$$

This enzyme is characterised by the complicated character of maximal enzyme activity dependence on pH. In the present case, we assumed that a part of the rate equation parameters should be depended on pH for correct taking into account this enzyme peculiarity.

$$K_{d\_Suc} = \frac{K^0_{d\_Suc}}{1 + H^+ \Big/ K_{h\_1} + K_{h\_2} \Big/ H^+};; K_{d\_Fum} = \frac{K^0_{ef\_Fum}}{1 + H^+ \Big/ K_{h\_3} + K_{h\_4} \Big/ H^+};$$

Here K_1 and K_2 are the dissociation constants for protons from the free enzyme form and from the enzyme complexes with succinate or coenzyme Q; K_3 and K_4 are the dissociation constants for protons from the enzyme complexes with fumarate or reduced coenzyme Q. Assumption of different affinity of protons with different enzyme forms and the introduction of 4 dissociation constants for protons were made on the basis of corresponding experimental data [96S], wherein initial velocities dependences on pH differed for forward and reverse reactions.

Parameter values and sources for verification are shown in table 32S.

Table 32S. Values of the SDH parameters.

Parameter	Value	Literature source
K_{eq_Sdh}	2250	Calculated from [101]
K_{m_Q}	0.002 mM	Estimated from [96S]
$K_{m\ QH2}$	0.0045 mM	Estimated from [96S]
K_{ef_Fum}	0.2 mM	Estimated from [97S]
K_{d_Suc}	0.01 mM	Estimated from [97S]
$K_{m\ Suc}$	0.28 mM	Estimated from [99S]
K_{m_Fum}	0.45 mM	Estimated from [100S]
K_{h_1}	1e-4 mM mM	Estimated from [96S]
$K_{h\ 2}$	5e-7 mM	Estimated from [96S]
$K_{h\ 3}$	8.5e-4 mM	Estimated from [96S]
$K_{h\ 4}$	1e-6 mM	Estimated from [96S]

Fumarase (FumA)

Fum catalyses reaction of reversible hydration, therefore this enzyme is described by reversible Michaelis-Menten equation.

$$V_{42} = \frac{V_{m\_Fum}\left(Fum - Mal/K_{eq\_Fum}\right)}{K_{m\_Fum} + Fum + Mal * K_{m\_Fum}/K_{m\_Mal}}$$

pH dependence of the enzyme activity was taken into account by the following changes in the rate equation:

$$k_{f\_Fum} = \frac{k_{f0\_Fum}}{1 + \frac{H}{K_{h\_3}} + \frac{K_{h\_4}}{H}};$$

$$K_{m\_Fum} = \frac{K_{m0\_Fum}(1 + \frac{H}{K_{h\_1}} + \frac{K_{h\_2}}{H})}{1 + \frac{H}{K_{h\_3}} + \frac{K_{h\_4}}{H}};$$

$$K_{m\_Mal} = \frac{K_{m0\_Mal}(1 + \frac{H}{K_{h\_1}} + \frac{K_{h\_2}}{H})}{1 + \frac{H}{K_{h\_3}} + \frac{K_{h\_4}}{H}}.$$

Parameter values and sources for verification are shown in table 33S.

Table 33S. Values of the Fum parameters.

Parameter	Value	Literature source
k_{f_Fum}	1.86e5 1/min	Estimated from [102S];
$k_{r\ Fum}$	4.02e04 1/min	Estimated from [102S];
K_{m_Fum}	0.6 mM	Estimated from [102S];
K_{m_Mal}	0.7 mM	Estimated from [102S];
K_{h_1}	0.0316 mM	Estimated from [102S];
K_{h_2}	5e-7 mM	Estimated from [102S];
K_{h_3}	1.26e-4 mM	Estimated from [102S];
K_{h_4}	3.98e-8 mM	Estimated from [102S];
K_{eq_Fum}	5.4	Estimated from [102S];

Malate dehydrogenase (Mdh)

This enzyme is coded by *mdh gene* and catalyses the reaction of malate oxidation. Rate equation was derived based on Ordered Bi Bi mechanism in accordance to Cleland's classification [103S]:

$$V_{44} = \frac{V_{m\_Mdh} * \left(NADH * OAA - NAD * Mal / K_{eq\_Mdh} \right)}{K_{i\_OAA} * K_{m\_NADH} + NADH * K_{m\_OAA} + K_{m\_NADH} * OAA + NADH * OAA + \\ + K_{i\_OAA} * K_{m\_NADH} * \left(NAD / K_{m\_NAD} * Mal / K_{m\_Mal} + NAD * Mal / K_{m\_NAD} * K_{m\_Mal} \right)}$$

Parameter values and sources for verification are shown in table 34S.

Table 34S. Values of the Mdh parameters.

Parameter	Value	Literature source
K_{eq_Mdh}	1e5	Estimated from [104S];
K_{i_OAA}	3mM	Estimated from [104S];
K_{m_NADH}	0.003mM	Estimated from [104S];
K_{m_OAA}	0.001mM	Estimated from [104S];
K_{m_Mal}	0.86mM	Estimated from [104S];
K_{m_NAD}	0.64mM	Estimated from [104S];

Malate dehydrogenase (Mqo)

This enzyme is coded by *mqo gene* and as well as Mdh catalyses the reaction of malate oxidation, but transfers electrons directly to the quinine pool of the respiratory chain without help of other cofactors. Unfortunately, there is a lack of quantitative experimental data for a detailed description of Mqo functioning. Therefore, we used the first level of detailing for the rate equation of this enzyme.

$$V_{43} = \frac{V_{m\_Mqo} * \left(Mal * Q - OAA * QH_2 / K_{eq\_Mqo} \right)}{K_{m\_Mal} * K_{m\_Q} + K_m * Mal + K_{m\_Mal} * Q + Mal * Q + \\ + K_{m\_Mal} * K_{m\_Q} * \left(OAA / K_{m\_OAA} + QH_2 / K_{m\_QH2} + OAA * QH_2 / K_{m\_OAA} * K_{m\_QH2} \right)}$$

Parameter values and sources for verification are shown in table 35S.

Table 35S. Values of the Mqo parameters.

Parameter	Value	Literature source
K_{eq_Mqo}	9	Taken from [105S];
K_{m_Mal}	0.435 mM	Taken from [105S];
K_{m_Q}	0.0414 mM	Taken from [105S];

K_{m_OAA}	10 mM	Free parameter;
K_{m_QH2}	10 mM	Free parameter;

Isocitrate lyase (AceA)

AceA is encoded by *aceA* gene, and it catalyses the reaction of glyoxylate and succinate formation from isocitrate. The rate equation was derived according to the Random Uni Bi mechanism with E-iCit-Suc dead complex and with inhibitors, namely, 3-phosphoglycerate (competitive to iCit) and phosphoenolpyruvate (non-competitive to iCit and Glx, competitive to Suc) [103S].

$$V_{45} = \frac{V_{m\_AceA} K_{m\_Glx} K_{d\_Suc} \left(iCit - Glx * Suc / K_{eq\_AceA} \right)}{K_{m\_iCit} K_{m\_Glx} K_{d\_Suc} \left(1 + PG / K_{d\_PG} + PEP / K_{d\_PEP} \right) + iCit * K_{m\_Glx} K_{d\_Suc} \left(1 + PEP / K_{eip\_PEP} \right) + + Suc * iCit * K_{m\_iCit} K_{m\_Glx} / K_{eis}^{iCit} + Glx * K_{m\_iCit} K_{m\_Suc} \left(1 + PEP / K_{egp\_PEP} \right) + Suc * K_{m\_iCit} * K_{m\_Glx} + + Glx * Suc * K_{m\_iCit}}$$

Parameter values and sources for verification are shown in table 36S.

Table 36S. Values of the AceA parameters.

Parameter	Value	Literature source
$k_{f\ AceA}$	1675 1/min	Estimated from [103S];
K_{m_iCit}	0.063mM	Estimated from [103S];
K_{m_Glx}	0.13mM	Estimated from [103S];
K_{m_Suc}	0.59mM	Estimated from [103S];
K_{d_PG}	0.8mM	Estimated from [103S];
K_{d_Suc}	0.53mM	Taken from [103S];
k_{r_AceA}	208 1/min	Taken from [103S];
K_{eis_iCit}	0.04mM	Taken from [103S];
K_{eip_PEP}	1.14mM	Taken from [103S];
K_{egp_PEP}	0.2mM	Taken from [103S];
K_{d_PEP}	1.05mM	Taken from [103S];
$V^{r}_{m\_AceA}$	0.993 mM/min	Estimated from [103S];
K_{eq_AceA}	8.8 mM	Estimated from [103S];

Malate synthase (AceB)

AceB is coded by *aceB* gene and catalyses the reaction of glyoxylate and acetyl-Coenzyme A bond with malate formation [106S]. Rate equation was derived according to Random Bi Bi mechanism.

$$V_{46} = \frac{V_{m\_AceB} * \left(Glx * AcCoA - Mal * CoA / K_{eq\_AceB} \right)}{K_{m\_Glx} * K_{m\_AcCoA} + K_{m\_AcCoA} * Glx + K_{m\_Glx} * AcCoA + Glx * AcCoA +};$$
$$+ K_{m\_Glx} * K_{m\_AcCoA} * \left(Mal / K_{m\_Mal} + CoA / K_{m\_CoA} + Mal * CoA / K_{m\_Mal} * K_{m\_CoA} \right)$$

Parameter values and sources for verification are shown in table 37S.

Table 37S. Values of the AceB parameters.

Parameter	Value	Literature source
K_{eq_aceB}	2.31e+05	Calculated [101S]
K_{m_Glx}	0.021 mM	Taken from [107S];
K_{m_AcCoA}	0.009 mM	Taken from [107S];
K_{m_Mal}	10 mM	Free parameter;
K_{m_CoA}	10 mM	Free parameter;

References

1S. Hoque MA, H.Ushiyama, Tomita M & Shimizu K (2005) Dynamic responses of the intracellular metabolite concentrations of the wild type and *pykA* mutant *Escherichia coli* against pulse addition of glucose or NH3 under those limiting continuous cultures. *Biochem Eng J* **26**, 38-49.

2S. Froschauer EM, Kolisek M, Dieterich F, Schweigel M & R.J.Schweyen (2004) Fluorescence measurements of free [Mg^{2+}] by use of mag-fura 2 in *Salmonella enterica*.

3S. Sundararaj S, Guo A, Habibi-Nazhad B, Rouani M, Stothard P, Ellison M & Wishart DS (2004) The CyberCell Database (CCDB): a comprehensive, self-updating, relational database to coordinate and facilitate in silico modeling of *Escherichia coli*. *Nucleic Acids Res* **32**, 293-295.

4S. Peng L & Shimizu K (2003) Global metabolic regulation analysis for Escherichia coli K12 based on protein expression by 2-dimensional electrophoresis and enzyme activity measurement. *Appl Microbiol Biotechnol* **61**, 163–178.

5S. Sprenger GA, Schorken U, Sprenger G & SAHM H (1995) Transketolase A of Escherichia coli K12. Purification and properties of the enzyme from recombinant strains. *Eur J Biochem* **232**, 525-532.

6S. Sprenger GA, Schorken U, Sprenger G & SAHM H (1996) Transaldolase B of Escherichia coli K12: Cloning of Its Gene, talB, and Characterization of the Enzyme from Recombinant Strains. *J Bacteriol* **177**, 5930–5936.

7S. Taquikhan MM & Martell AE (1962) Metal chelates of adenosine triphosphate. *J Phys Chem* **66**, 10-15.

8S. Chassagnole C, Noisommit-Rizzi N, Schmid JW, Mauch K & Reuss M (2002) Dynamic modeling of the central carbon metabolism of *Escherichia coli*. *Biotechnol Bioenerg* **79**, 53-73.

9S. Postma PW, Lengeler JW & Jacobson GR (1995) Phosphoenolpyruvate:Carbohydrate Phosphotransferase Systems. In *Escherichia coli and Salmonella: Cellular and Molecular Biology* (Neidhardt FC, Curtis R, Ingraham JL, Lin ECC, Low KB, Magasanik B, Reznikoff WS, Riley M, Schaechter M & Umbargo HE, eds), pp. 1149-1175. ASM Press, Washington DC.

10S. Peskov KV, Goryanin II & Demin OV (2008) Kinetic Model of Phosphofructokinase-1 from *Escherichia coli*. *J Bioinform Comp Biol* **6**, 843-867.

11S. Peskov K & Demin O (2010) Kinetic model of phosphofructokinase-2 from *Escherichia coli*. *Voprosi Bio Med Pharm Chem* **5**, 11-22.

12S. Ferenci T (1996) Adaptation to life at micromolar nutrient levels: the regulation of Escherichia coli glucose transport by endoinduction and cAMP. *FEMS Microbiol Rev* **18**, 301-317.

13S. Nelson DL & Cox MM (2005) *Lehninger. Principles of Biochemistry. 4th edition.* W.H.Freeman and Company, New York.

14S. Meyer D, Schneider-Fresenius C, Horlacher R & Peist R (1997) Molecular Characterization of Glucokinase from Escherichia coli K-12. *J Bacteriol* **179**, 1298–1306.

15S. Ogawa T, Mori H, Tomita M & Yoshino M (2007) Inhibitory effect of phosphoenolpyruvate on glycolytic enzymes in Escherichia coli. *Res Microbiol* **158**, 159-163.

16S. Marchaud M, Kooystra U, Wierenga RK, A.-M. Lambetr, Beeumen JV, Opperdoes FR & Michels PAM (1989) Glucosephosphate isomerase from Trypanosoma brucei. Cloning and characterization of the gene and analysis of the enzyme. *Eur J Biochem* **184**, 455-464.

17S. Schreyer R & Bock A (1980) Phosphoglueose Isomerase from Escherischia coli KI2: Purification, Properties and Formation under Aerobicand Anaerobic Condition. *Arch Microbiol* **127**, 289-298.

18S. Babul J, Clifton D, Kretschmer M & Fraenkel DG (1993) Glucose metabolism in Escherichia coli and the effect of increased amount of aldolase. *Biochemistry* **32**, 4685-4692.

19S. Baldwin SA, Perham RN & Stribling D (1978) Purification and Characterization of the Class-Il D-Fructose-1,6-Bisphosphate Aldolase from Escherichia coli (Crookes' Strain). *Biochem J* **169**, 633-641.

20S. Plater AR, Zgiby SM, Thomson GJ, Qamar S, Wharton CW & Berry A (1999) Conserved Residues in the Mechanism of the E. coli Class II FBP-aldolase. *J Mol Biol* **285**, 843-855.

21S. Nojima H, Oshima T & Noda H (1979) Purification and properties of phosphoglycerate kinase from Thermus thermophilus strain HB8. *J Biochem* **85**, 1509-1517.

22S. Kuntz GW & Krietsch WK (1982) Phosphoglycerate kinase from spinach, blue-green algae, and yeast. *Methods Enzymol* **90**, 110-114.

23S. Cleland WW (1963) The kinetics of enzyme-catalyzed reactions with two or more substrates and products. I. Nomencluture and rate equations. *Biochim Biophys Acta* **67**, 104-137.

24S. D'Alessio G & Josse J (1971) Glyceraldehyde Phosphate Dehydrogenase of Escherichia coli. Structural and catalytic properties. *J Biol Chem* **246**, 4326-4333.

25S. Eyschen J, Vitoux B, Marraud M, Cung MT & Branlant G (1999) Engineered Glycolytic Glyceraldehyde-3-Phosphate Dehydrogenase Binds the Anti Conformation of NAD1 Nicotinamide but Does Not Experience A-Specific Hydride Transfer. *Arch Biochem Biophys* **364**, 219–227.

26S. Lambier A-M, Loiseau AM, Kuntz DA, Vellieux FM, Michels PAM & Opperdoes FR (1991) The cytosolic and glycosomal glyceraldehyde-3-phosphate dehydrogenase from Trypanosoma brucei. Kinetic properties and comparison with homologous enzymes. *Eur J Biochem* **198**, 429-435.

27S. Watabe K & Freese E (1979) Purification and Properties of the Manganese-Dependent Phosphoglycerate Mutase of Bacillus subtilis. *J Bacteriol* **137**, 773-778.

28S. Spring TG & Wold F (1971) The Purification and Characterization of Elscherichia coli Enolase. *J Biol Chem* **246**, 6797-6802.

29S. Munoza ME & Ponce E (2003) Pyruvate kinase: current status of regulatory and functional properties. *Comp Biochem Physiol Part B* **135**, 197–218.

30S. Waygood EB & Sanwal BD (1974) The control of pyruvate kinases of Escherichia coli. I. Physicochemical and regulatory properties of the enzyme activated by fructose 1,6-diphosphate. *J Biol Chem* **249**, 265-274.

31S. Waygood EB, Rayman MK & Sanwal BD (1975) The control of pyruvate kinases of Escherichia coli. II. Effectors and regulatory properties of the enzyme activated by ribose 5-phosphate. *Can J Biochem* **53**, 444-454.

32S. Mort JS & Sanwal BD (1978) The control of pyruvate kinases of Escherichia coli: further studies of the enzyme activated by ribose-5-phosphate. *Can J Biochem* **56**, 647-653.

33S. Gibriel AY & Doelle HW (1975) Investigation into pyruvatekinases of Escherichia coli K12 grown underaerobic and unaeribic conditions. *Microbios* **12**, 179-197.

34S. Waygood EB & Sanwal BD (1972) Regulation of pyruvatekinases by succinyl CoA. *Biochem Biophys Res Commun* **48**, 402-407.

35S. Valentini G, Chiarelli L, Fortin R, Speranza ML, Galizzi A & Mattevi A (2000) The Allosteric Regulation of Pyruvate Kinase. *J Biol Chem* **275**, 18145–18152.

36S. Hino Y & Minakami S (1982) Hexose-6-Phosphate and 6-Phosphogluconate Dehydrogenases of Rat Liver Microsomes. Involvement in NADPH and Carbon Dioxide Generation in the Luminal Space of Microsomal Vesicles. *J Biochem* **92**, 547-557.

37S. Ivanicky G, Krinsky V & Sel'kov E (1978) *Mathematical Biophysics of the Cell* Nauka, Moscow.

38S. Popova SV & Sel'kov EE (1975) Generalization of the model by Monod, Wyman and Changeux fro the case of reversible monosubstrate reaction S↔P. *FEBS Lett* **53**, 269-273.

39S. Popova SV & Sel'kov EE (1976) A generalization of the Monod-Wyman-Changeux model for the case of multisubstrate reactions. *Mol Biol (Moscow)* **10**, 1116-1126.

40S. Popova S & Sel'kov E (1978) Regulatory reversible enzymic reactions. Theoretical analysis. *Mol Biol (Moscow)* **12**, 1139-1151.

41S. Miclet E, Stoven V, Michels PAM, Opperdoes FR, Lallemand J-Y & Duffieux F (2001) NMR Spectroscopic Analysis of the First Two Steps of the Pentose-Phosphate Pathway Elucidates the Role of 6-Phosphogluconolactonase. *J Biol Chem* **276**, 34840–34846.

42S. Banerjee S & Fraenkel DG (1972) Glucose-6-Phosphate Dehydrogenase from Escherichia coli and from a "High-Level" Mutant. *J Bacteriol* **110**, 155-160.

43S. Sanwal BD (1970) Regulatory mechanisms involving nicotinamide adenine nucleotides as allosteric effectors. 3. Control of glucose 6-phosphate dehydrogenase. *J Biol Chem* **245**, 1626-1631.

44S. Glaser L & Brown DH (1955) Purification and properties of D-Glucose-6-Phosphate dehydrogenase. *J Biol Chem* **216**, 67-79.

45S. Clarke JL & Mason PJ (2003) Murine hexose-6-phosphate dehydrogenase: a bifunctional enzyme with broad substrate specificity and 6-phosphogluconolactonase activity. *Arch Biochem Biophys* **415**, 229-234.

46S. Scopes RK (1985) 6-Phosphogluconolactonase from Zymomonas mobolis. An enzyme of high catalytic efficiency. *FEBS Lett* **193**, 185-188.

47S. Silva AOd & Fraenkel DG (1979) The 6-Phosphogluconate Dehydrogenase Reaction in Escherichia coli. *J Biol Chem* **254**, 10237-10242.

48S. Horecker BL & Hurwitz J (1956) The purification of phosphoketopentoepimerase from Lactobacillus pentosus and the preparation of xylulose 5-phosphate. *J Biol Chem* **223**, 993-1008.

49S. Villet RH & Dalziel K (1969) The Nature of the Carbon Dioxide Substrate and Equilibrium Constant of the 6-Phosphogluconate Dehydrogenase Reaction. *Biochem J* **115**, 633-638.

50S. Woodruff WW & Wolfenden R (1979) Inhibition of Ribose-5-phosphate Isomerase by 4-Phosphoerythronate. *J Biol Chem* **254**, 5866-5867.

51S. Domagkk GF, Doering M & Chilla R (1973) Purification and Properties of Ribose-Phosphate Isomerase from Candida utilis. *Eur J Biochcm* **38**, 259-264.

52S. Zhang R, Andersson CE, Savchenko A, Skarina T, Evdokimova E, Beasley S, Arrowsmith CH, Edwards AM, Joachimiak A & Mowbray SL (2003) Structure of Escherichia coli Ribose-5-Phosphate Isomerase: A Ubiquitous Enzyme of the Pentose Phosphate Pathway and the Calvin Cycle. *Structure* **11**, 31-42.

53S. Selivanov VA, Meshalkina LE, Solovjeva ON, Kuchel PW, Ramos-Montoya A, Kochetov GA, Lee PW-N & Cascante M (2005) Rapid simulation and analysis of isotopomer distributions using constraints based on enzyme mechanisms: an example from HT29 cancer cells. *Bioinformatics* **21**, 3558–3564.

54S. Casazza JP & Veech RL (1985) The Interdependence of Glycolytic and Pentose Cycle Intermediates in Libitum Fed Rats. *J Biol Chem* **261**, 690-698.

55S. Datta AG & Racker E (1961) Mechanism of action of Transketolase. *J Biol Chem* **236**, 617-623.

56S. Kuhn E & Brand K (1972) Purification and properties of transaldolase from bovine

57S. Horecker BL, Cheng T & Pontremoli S (1963) The Coupled Reaction Catalyzed by the Enzymes Transketolase and Transaldolase. *J Biol Chem* **238**, 3428-3431.

58S. Wood WA (1971) 6-Phosphoglucponic and related dehydrases. In *The Enzymes, 3rd Ed* (Boyer PD, ed^eds), pp. 573-586.

59S. Cheriyan M, Toone EJ & Fierke CA (2007) Mutagenesis of the phosphate-binding pocket of KDPG aldolase enhances selectivity for hydrophobic substrates. *Protein Sci* **16**, 2368-2377.

60S. Torres JC, Guixe V & Babul J (1997) A mutant phosphofructokinase produces a futile cycle during gluconeogenesis in *Escherichia coli*. *Biochem J* **327**, 675-684.

61S. Hines JK, Kruesel E, Fromm HJ & Honzatko RB (2007) Structure of Inhibited Fructose-1,6-bisphosphatase from Escherichia coli. *J Biol Chem* **282**, 24697–24706.

62S. Choe J-Y, Nelson SW, Arienti KL, Axe FU, Collins TL, Jones TK, Kimmich RDA, Newman MJ, K.Norvell, Ripka WC, Romano SJ, Short KM, Slee DH, Fromm HJ & Honzatko RB (2003) Inhibition of Fructose-1,6-bisphosphatase by a New Class of Allosteric Effectors. *J Biol Chem* **278**, 51176–51183.

63S. Hines JK, Fromm HJ & Honzatko RB (2006) Novel Allosteric Activation Site in Escherichia coli Fructose-1,6-bisphosphatase. *J Biol Chem* **281**, 18386–18393.

64S. Kelley-Loughnane N, Biolsi SA, Gibson KM, Lu G, Hehir MJ, Phelan P & Kantrowitz ER (2002) Purification, kinetic studies, and homology model of Escherichia coli fructose-1,6-bisphosphatase. *Biochim Biophys Acta* **1594**, 6-16.

65S. Fraenkel DG, Pontremoli S & Horecker BL (1966) The specific fructose diphosphatase of E. coli: Properties and partial purification. *Arch Biochem Biophys* **114**, 4-12.

66S. Babul J & Guixe V (1983) Fructose bisphosphatase from Escherichia coli. Purification and characterization. *Arch Biochem Biophys* **225**, 944-949.

67S. Marcus F, Edelstein I & Rittenhouse J (1984) Inhibition of E. coli FbP by Fru-2,6-P. *Biochem Biophys Res Commun*, 1103-1108.

68S. Parducci RE, Cabrera R, Baez M & Guixe V (2006) Evidence for a Catalytic Mg^{2+} Ion and effect of Phosphate on the Activity of Escherichia coli Phosphofructokinase-2: Regulatory Properties of a Ribokinase Family Member *Biochemistry* **45**, 9291-9299.

69S. Donahue JL, Bownas JL, Niehaus WG & Larson TJ (2000) Purification and Characterization of glpX-Encoded Fructose-1,6-Bisphosphatase, a New Enzyme of the Glycerol-3-Phosphate Regulon of Escherichia coli. *J Bacteriol* **182**, 5624–5627.

70S. Chulavatnatol M & Atkinson DE (1973) Phosphoenolpyruvate Synthetase from Escherichia coli. Effects of adenylate ekergy charge and modifier concentrations. *J Biol Chem* **248**, 2712-2715.

71S. Mogilevskaya EA, Lebedeva GV, Goryanin IL & (Moscow) OVDB (2007) Kinetic model of Escherichia coli isocitrate dehydrogenase functioning and regulation. *Biophysics (Moscow)* **52**, 47-56.

72S. Berman KM & Cohn M (1970) Phosphoenolpyruvate Synthetase of Escherichia coli. Purification, some properties, and the role of divalent metal ions. *J Biol Chem* **245**, 5309-5318.

73S. Cooper RA & Kornberg HL (1967) The direct synthesis of phosphoenolpyruvate from pyruvate by E. coli. *Proc Roy Soc* **B163**, 263-280.

74S. Wricht JA & Sanwal BD (1969) Regulatory Mechanisms Involving Nicotinamide Adenin Nucleotides as Allosteric Eff ectors. *II Control of phosphoenolpyruvate carboxykinase* **244**, 1838-1845.

75S. Krebs A & Bridger WA (1980) The kinetic propeties of PckA from E. coli. *Can J Biochem* **58**, 309-318.

76S. Corwin LM & Fanning GR (1968) Studies of parameters affecting the allosteric nature of phosphoenolpyruvate carboxylase. *J Biol Chem* **243**, 3517-3525.

77S. Wohl RC & Markus G (1972) Phosphoenolpyruvate carboxylase of E. coli. Purification and some properties. *J Biol Chem* **247**, 5785-5792.

78S. Gold EW & Smith TE (1974) Escherichia coli phosphoenolpyruvate carboxylase: effect of allosteric inhibitors on the kinetic parameters and sedimentation behavior. *Arch Biochem Biophys* **164**, 447-455.

79S. Bologna FP, Andreo CS & Drincovich MF (2006) Escherichia coli Malic Enzymes: Two Isoforms with Substantial Differences in Kinetic Properties, Metabolic Regulation, and Structure. *J Bacteriol* **189**, 5937–5946.

80S. Sanwal BD (1970) Regulatory characteristic of the diphosphopyridine nucleotide-specific malic enzyme of E. coli. *J Biol Chem* **245**, 1212-1216.

81S. Milne JA & Cook RA (1979) Role of metal cofactors in enzyme regualation. Differences in the regulatory properties of E. coli NAD specific malic enzyme depending on hwether Ng or Mn serves as divalent cation. *Biochemistry* **18**, 3604-3610.

82S. Yamaguchi M (1979) Studies on regulatory functions of Malic enzymes. *J Biochem* **86**, 325-333.

83S. Sanwal BD & Smando R (1969) Malic enzyme of E.coli. Diversity of the effectors controling enzyme activity. *J Biol Chem* **244**, 1817-1823.

84S. Sanwal BD & Smando R (1969) Malic enzyme of E.coli. Possible mechanism for allosteric effects. *J Biol Chem* **244**, 1824-1830.

85S. Brown DA & Cook RA (1981) Role of metal cofactors in enzyme regulation. *Biochemistry* **20**, 2503-2512.

86S. Sanwal BD, Wright JA & Smando R (1968) Allosteric control of the activity of malic enzyme in E. coli. *Biochem Biophys Res Commun* **31**, 623-627.

87S. Tang Y, Quail MA, Artymiuk PJ, Guest JR & Green J (2002) Escherichia coli aconitases and oxidative stress: post-transcriptional regulation of sodA expression. *Microbiology* **148**, 1027–1037.

88S. Varghese S, Tang Y & Imlay JA (2003) Contrasting Sensitivities of Escherichia coli Aconitases A and B to Oxidation and Iron Depletion. *J Bacteriol* **185**, 221–230.

89S. Woods SA, Schwartzbach SD & Guest JR (1988) Two biochemically distinct classes of fumarase in Escherichia coli. *Biochim Biophys Acta* **954**, 14-26.

90S. Mogilevskaya EA, Lebedeva GV & Demin OV (2006) Kinetic model of E. coli 2-ketoglutarate dehydrogenase functioning. *Russian Biomedical Journal* **7**, 442-449.

91S. Tarmy EM & Kaplan NO (1967) Kinetics of Escherichia coli B D-Lactate Dehydrogenase and Evidence for Pyruvate-controlled Change in Conformation. *J Biol Chem* **243**, 2587-2596.

92S. Kale S, Arjunan P, Furey W & Jordan F (2007) A dynamic loop at the active center of the Escherichia coli pyruvate dehydrogenase complex E1 component modulates substrate utilization and chemical communication with the E2 component. *J Biol Chem* **282**, 28106-28116.

93S. Jordan PA, Tang Y, Bradbury AJ, Thomson AJ & Guest JR (1999) Biochemical and spectroscopic characterization of E.coli aconitases (AcnA and AcnB). *Biochem J* **344**, 739-746.

94S. Miller SL & Smith-Magowan D (1990) The thermodynamics of the Krebs cycle and related compounds. *J Phys Chem* **19**, 1049-1073.

95S. Waskiewicz DE & Hammes GG (1984) Elementary steps in the reaction mechanism of the alpha-ketoglutarate dehydrogenase multienzyme complex from Escherichia coli: kinetics of succinylation and desuccinylation. *Biochemistry* **23**, 3136-3143.

96S. Amarasingham CR & Davis BD (1965) Regulation of alpha-ketoglutarate dehydrogenase formation in Escherichia coli *J Biol Chem* **240**, 3664-3668.

97S. Maklashina E & Cecchini G (1999) Comparison of Catalytic Activity and Inhibitors of Quinone Reactions of Succinate Dehydrogenase (Succinate-Ubiquinone Oxidoreductase) and Fumarate Reductase (Menaquinol-Fumarate Oxidoreductase) from Escherichia coli. *Biochemistry* **36**, 223-232.

98S. Kotlyar AB & Vinogradov AD (1984) Dissociation constants of the succinate dehydrogenase complexes with succinate, fumarate and malonate. *Biochemistry (Moscow)* **49**, 511-518.

99S. Kim IC & Bragg PD (1971) Some properties of the Succinate Dehydrogenase of Escherichia coli. *Can J Biochem* **49**, 1098-1104.

100S. Hirsch CA, Rasminsky M, Davis BD & Lin EC (1963) A fumarate reductase in Escherichia coli distinct from succinate dehydrogenase *J Biol Chem* **238**, 3770-3774.

101S. Alberty RA (2000) Calculating apparent equilibrium constants of enzyme-catalyzed reactions at pH 7. *Biochem Education* **28**, 12-17.

102S. Murphey WH & Kitto GB (1969) Malate Dehydrogenase from E.coli *Methods Enzymol* **13**, 145-147.

103S. MacKintosh C & Nimmo HG (1988) Purification and regulatory properties of isocitrate lyase from Escherichia coli ML308. *Biochem J* **250**, 25-31.

104S. Wright SK, Zhao FJ, Rardin J, Milbrandt J, Helton M & Furumo NC (1995) Mechanistic studies on malate dehydrogenase from Escherichia coli *Arch Biochem Biophys* **321**, 289-296.

105S. Molenaar D, Rest MEVd & Petrovic S (1998) Biochemical and genetic characterization of the membrane-associated malate dehydrogenase (acceptor) from Corynebacterium glutamicum. *Eur J Biochem* **254**, 395-403.

106S. Howard BR, Endrizzi JA & Remington SJ (2000) Crystal structure of Escherichia coli malate synthase G complexed with magnesium and glyoxylate at 2.0 A resolution: mechanistic implications. *Biochemistry* **39**, 3156-3168.

107S. Falmagne P & Wiame JM (1973) Purification and partial characterization of two malate synthases of Echerichia coli. *Eur J Biochem* **37**, 415-424.